Science Immunology
AAAS

Supplementary Materials for

A multimorphic mutation in IRF4 causes human autosomal dominant combined immunodeficiency

IRF4 International Consortium

Corresponding author: Anselm Enders, anselm.enders@anu.edu.au; Sven Kracker, sven.kracker@inserm.fr; Ruben Martinez-Barricarte, ruben.m.barricarte@vumc.org; Stephan Mathas, stephan.mathas@charite.de; Sergio D. Rosenzweig, srosenzweig@cc.nih.gov; Klaus Schwarz, klaus.schwarz@uni-ulm.de; Stuart E. Turvey, sturvey@bcchr.ca; Ji-Yang Wang, wang@ fudan.edu.cn

Sci. Immunol. **8**, eade7953 (2023)
DOI: 10.1126/sciimmunol.ade7953

The PDF file includes:

Materials and Methods
Figs. S1 to S9
Tables S1 to S13
References (*66*–*77*)

Other Supplementary Material for this manuscript includes the following:

Data files S1 to S4
MDAR Reproducibility Checklist

Supplementary Materials

Supplemental Materials and Methods

RNA isolation and RT-PCR

Total RNA of 500 activated naïve $CD4^+$ T cells was isolated and reverse transcribed by the CellLyse Microlysis and cDNA Synthesis Kit (TATAA Biocenter AB, Sweden). Primers used for the PCR amplification of IRF4 and ACTB cDNAs were listed in Table S13.

Flow cytometry

Flow cytometric phenotyping was performed either by using 100 µl fresh, heparinized full blood or cryopreserved PBMC. For surface staining, single cell suspensions were first incubated with either human BD Fc block or anti-mouse CD16/32 antibody on ice to block human or mouse FcγR and then stained with fluorophore-conjugated antibodies. 7-AAD Viability Staining Solution (eBioscience, Thermo Fisher Scientific) was used for live versus dead cell discrimination. For determination of regulatory T cells (Treg) by intracellular staining of FOXP3, we used the Human Regulatory T Cell Staining Kit from eBioscience (Thermo Fisher Scientific, USA) according to the manufacturers' instructions. For IRF4 intracellular staining, PBMCs were fixed and permeabilized after T and B surface marker staining using FoxP3 staining kit (eBioscience) according to the manufacturer's instructions. Cells were incubated with an Alexa Fluor® 647 anti-IRF4 Antibody (Biolegend) on ice for 30 min. Cells were washed with the staining buffer.

Th1, Th2 and Th17 cells of P5-P7 were detected by intracellular staining of cytokines: PBMC ($1x10^6$/ml) were either left unstimulated or stimulated with 10 ng/ml or 100 ng/ml PMA (Phorbol-12-Myristat13-Acetate) and 1 µg/ml Calcium-Ionophore (Merck, Germany) under addition of 1 µg/ml Brefeldin A (BD Biosciences, USA) for 6 or 12 h at 37°C. Cells then were harvested and washed twice with PBS/1% FCS. For surface staining, cells were incubated with anti-CD45RO-PE, anti-CD3-APC, anti-CD4-APCAlexaFluor750 and anti-CD45-KromeOrange or anti-CD3-PerCP and anti-CD4-PEcy7 for 30 min at 4°C. After being washed twiced with PBS/1% FCS, cells were fixed and permeabilized with 100 µl Cytofix/ CytopermTM (BD Biosciences, USA). For intracellular staining, cells were incubated with anti-IFNγ, anti-IL4 and anti-IL17A and anti-CD4 for 45 min at 4°C. Cells were washed twice with Perm/Wash Buffer (BD Biosciences, USA) and diluted in 500 µl PBS/1% FCS.

Samples were analyzed with a FACSVerse flow cytometer (BD Biosciences), a NaviosTM Flow Cytometer (Beckman Coulter, USA), a FACS Canto II flow or a Fortessa LSR cytometer (BD Biosciences, USA). Data analysis was performed using FlowJo software (BD Biosciences, USA).

Immunoblot

Whole-cell lysates extracted with medium radioimmunoprecipitation assay (RIPA) lysis buffer (Cwbiotech) and cytoplasmic and nuclear lysates extracted with Nuclear and Cytoplasmic Protein Extraction Kit (Sangon Biotech) were resolved by sodium dodecyl sulfate polyacrylamide gel electrophoresis (SDS-PAGE) and transferred to an immobilon-P membrane (MILLIPORE). Immunoblots were performed with specific primary antibodies overnight at 4℃ followed by horseradish peroxidase (HRP)-conjugated secondary antibodies for 1 h at room temperature and developed with an enhanced chemiluminescence light (ECL) reagent (MILLIPORE). For immunoblotting in T cell blasts, total PBMCs were stimulated with anti-CD3 and anti-CD28 antibodies in the presence of IL2 (10 ng/ml) for 10 days. Fresh IL2 was added every 2-3 days. T cell blasts were washed with PBS once and lysed in the lysis buffer (50mM Tris pH 7.4, 150mM

NaCl, 2mM EDTA, 0.5% Triton X-100 and 0.5% NP40 and protease and phosphatase inhibitor cocktail [Sigma, PPC1010]). Cell lysates were subjected to the immunoblotting.

Evaluation of cell proliferation

Total PBMCs were incubated with CellTrace violet Cell Proliferation Kit (1μM; Invitrogen) according to manufacturer's instructions. Cells were stimulated with anti-CD3 antibody and anti-CD28 antibodies (1 μg/mL each, eBioscience) for four days. For B cell proliferation, cells were stimulated with indicated agonists; anti-IgM (10 μg/ml, Jackson Lab), CD40L (100ng/ml, Enzo), IL4 (50 ng/ml, Peprotech), CpG (500 nM, Enzo) for four days. Cells were stained with fluorochrome-conjugated CD4, CD8, or CD19 antibodies (BD Biosciences, Clone RPA-T4, RPA-T8, HIB19 respectively) for 30 minutes at 4°C (dark). Cells were washed with PBS twice, and cells were acquired and analyzed by flow cytometry (Becton Dickinson FACSCanto II) and FlowJo software (FlowJo 10.5.2, TreeStar).

Enzyme linked immunosorbent assay (ELISA)

Human IgM and IgG levels in culture supernatants were measured as described (*66*) or measured by ELISA kits (Abcam; Cat# ab195215, ab214568, ab196263). IL2 and IFNγ cytokine production was analyzed by ELISA (Thermo Fisher Scientific) according to the manufacturer's instructions. Levels of mouse IgA, IgM, IgG, IgG_1, IgG_{2b}, IgG_{2c}, and IgG_3 and IgM and IgG1 in serum or culture supernatants were measured by ELISA performed as described previously (*49*). Levels of CXCL13 in patient and healthy controls sera were measured using the Quantikine ELISA Human CXCL13/BLC/BCA-1 Kit (R&D Systems; USA).

Flow cytometry for TCR Vbeta repertoire analysis

The Vβ T-cell repertoire was evaluated according to the manufacturer's instructions with the Beta Mark TCR Vbeta Repertoire Kit (Beckman-Coulter, USA), which allows detection of 24 different Vβ T-cell receptors.

NK-cell degranulation (CD107a assay)

Cryopreserved PBMCs ($2x10^6$/ml) were thawed, washed and incubated overnight at 37°C in either cell-culture medium (RPMI/ 10% FCS, PAN Biotech, 1% Penicillin/Streptomycin, 14 mM Hepes, and 2 mM L-Glutamin (Gibco/Thermo Fisher Scientific, USA), alone or in medium supplemented with 600 U/ml IL2 (PeproTech/tebu-bio, Germany). After harvesting and washing, 100 µl ($2x10^5$) of cells were cocultivated with 100 µl ($2x10^5$) K562 cells (DSMZ, Germany) or 100 µl of medium alone after adding of 5 µl/well anti-CD107a FITC in a 96 well U-bottom plate for 2.5 h at 37°C. Cells were stained with anti-CD107a FITC, anti-CD56 ECD, anti-CD3 APC and CD45 Krome Orange. Samples were acquired in 500 µl IF-Medium with a NaviosTM Flow Cytometer and analyzed with the NaviosTM 1.2. Software (Beckman Coulter, USA).

CD8 T-cell degranulation (CD107a assay)

Cryopreserved PBMCs ($1x10^6$/ml) were thawed, washed and cultured in cell-culture medium with 100 U/ml IL2 and with or without adding of 2% PHA (Gibco/Thermo Fisher) for 4 days at 37°C. After harvesting and washing, $2x10^5$ cells/200 µl were either restimulated with 15 µl CD3/CD28 beads (Gibco/ Thermo Fisher Scientific, USA) or incubated in culture-medium alone after adding of 5 µl/well anti-CD107a FITC in a 96 well U-bottom plate for 3 h at 37°C. Cells were then stained with anti-CD107a FITC, CD3 APC, CD8 Pacific Blue, CD45 Krome Orange. Samples were acquired in 500 µl IF-Medium with a NaviosTM Flow Cytometer (Beckman Coulter, USA) and analyzed with the NaviosTM 1.2. Software (Beckman Coulter, USA).

Construction of IRF4-expression vectors and plasmid transfection, and retrovirus and lentiviral transduction

Amplification of WT and T95R IRF4 cDNA was performed with KOD-plus polymerase (TOYOBO) using the first-strand cDNA generated from total RNA of PBMC from the patient and HC. Primers were listed in Table S13. The PCR products were inserted into pFlag-CMV-5a (Sigma-Aldrich) expression vector, pMX-IRES-GFP and pMX-IRES-hCD8a retroviral vectors. To generate the pcDNA3-FLAG-JUNB and pcDNA3-FLAG-BATF expression constructs, full length human JUNB and BATF were amplified from cDNA of the human cell line L428, and cloned via BamHI and XhoI into pcDNA3-FLAG (Invitrogen). The pHEBO-IRF4-HAtag expression construct and its empty control pHEBO-CMV-HAtag were kindly provided by L. Pasqualucci (New York, USA). The c.284C>G mutation was introduced into the pHEBO-IRF4-HAtag construct by use of the QuikChange Multi Site-Directed Mutagenesis Kit (Stratagene). For the retroviral transduction experiments of the C57BL/6 splenic B cells, the coding sequences for human IRF4 (WT or T95R) were amplified from the pHEBO-constructs using the IRF4_XhoI_forw 5′- ACC TCG AGG CCA CCA TGA ACC TGG AGG GCG GCG GCC GA - 3′and the IRF4_EcoRI_rev 5′- ACG AAT TCT TAA GGC CCT GGA CCC AAA GAA GCG TAA TC - 3′ primers and cloned in front of the IRES sequence of the MSCV-IRES-GFP (MIG) plasmid (a kind gift of F. Rosenbauer, Münster, Germany) via XhoI and EcoRI. All constructs were verified by sequencing.

Each retroviral construct was transfected either into Ampho or PlatE packaging cells (*67*) and the virus supernatants collected after 48 h and 72 h were filtered and concentrated with PEG8000. Virus transduction of Raji, Ramos, IRF4-deficient Ramos (clone 1-9 and 2-2), and CH12 cells was carried out in the presence of 8 μg/ml polybrene reagent (Sigma). For mouse splenic B cell transduction, purified B cells (density: $1x10^6$ cells/mL; $4x10^6$ cells per well) were cultured in the presence of recombinant mouse IL4 (25 ng/ml) and LPS (20 μg/ml) over night. 24 h after isolation, B cells were collected (300g, 5min, 4°C) and resuspended in B cell medium supplemented with 8 μg/mL polybrene (EMD Millipore, #TR-1003) at a density of $2x10^6$ cells/ml. To introduce WT and T95R IRF4, $4x10^6$ B cells per well were plated in 2 ml on 6-well plates that had been coated with RetroNectin (Takara, #T100B; 25 μg/mL; 4°C, overnight), blocked with 2% BSA (in PBS, 1h, RT) and pre-loaded with the respective retroviral particles (1 h, 37°C). Retroviral transduction was performed by the addition of 2 ml of the respective retroviral supernatant and subsequent centrifugation (800g, 90min, 32°C). 24 h after transduction, B cells were collected (300g, 5min, 4°C), resupended in new B cell medium and cultured (density: $1x10^6$ cells/ml; $4x10^6$ cells per well) for another 72 h (FACS for RNA-seq, flow cytometric analysis of plasma cell differentiation) in the presence of recombinant mouse IL4 (25 ng/ml) and LPS (20 μg/ml).

For transient transfection of 293T cells, Opti-MEM (GIBCO) and Hieff Trans™ Liposomal Transfection Reagent (YEASEN) were used following the company's protocol. For analysis of luciferase activity, HEK293 cells were transfected by electroporation in OPTI-MEM I using Gene-Pulser II (Bio-Rad) with 960 μF and 0.18 kV with 5 μg of pGL3-based reporter constructs, together with 150 ng pRL-TKLuc as an internal control. Where indicated, cells were additionally transfected with 5 μg pcDNA3-FLAG-JUNB, 5 μg pcDNA-FLAG-BATF, or 40 μg of the respective pHEBO-IRF4 variants. 48 hours after transfection, the ratio of the two luciferases was determined (Dual luciferase kit; Promega).

Surface plasmon resonance

- Protein Expression and purification

Codon-optimised gene constructs of IRF4^{WT} and IRF4^{T95R} DBD domains were cloned into pJ411KanR (ATUM) plasmids and transformed into *E. coli* BL21 (DE3) (Novagen) for expression as an N-terminal His_6 tag-fusion protein. Bacterial cultures were grown up in 2X YT media with over expression of constructs induced at 18 °C with 0.6mM IPTG. Following overnight incubation, cell pellets were suspended in 50 mM sodium phosphate buffer (pH 7.0), 500 mM NaCl and 30 mM imidazole (Buffer A) supplemented with protease inhibitor cocktail (Sigma), 3 mM β-mercaptoethanol, 0.5% Triton X-100, 4 mM MgCl2 and lysed via French press at 1500 psi. The DBD proteins were purified via Nickle affinity purification using a 5 ml HisTrap column (Cytiva) in Buffer A, against a linearly increasing imidazole gradient of up to a concentration of 500 mM.

Following isolation, the N-terminal His_6 tag was cleaved from DBD using overnight HRV3c digestion at 4 °C. Through a second round of Nickle affinity purification (as previously described), IRF4^{WT} and IRF4^{T95R} DBD proteins were isolated from the cleaved His tags. Further purification of IRF4^{WT} and IRF4^{T95R} DBD proteins were achieved via size exclusion chromatography (SEC) using a superdex 200 16/600 gel filtration column (Cytiva) in a 20 mM Tris buffer (pH 7.4), 150 mM NaCl, 1 mM TCEP buffer.

- Affinity determination

Affinity values of both IRF4 DBD constructs were acquired on a Biacore 8K (Cytiva) at 20°C with HBS buffer (10 mM HEPES-HCl, pH 7.4, and 150 mM NaCl) with additional 3 mM ETDA and 0.05 % P20 used as the running buffer. The biotinylated DNA motifs of interest (ISRE, EICE1, AICE1, and AICE2) (Integrated DNA technologies) were immobilised (up to ~ 2,000 RU) on a Series S streptavidin (SA) chip (Cytiva) as per manufacturer's instructions. Affinity measurements were gained by passing serially increasing concentrations of IRF4^{WT} and IRF4^{T95R} DBD proteins (up to 5 µM) over each of the coupled DNA motifs at a flow rate of 30 µl/min. The final response unit was calculated by subtracting the response unit of the reference flow cell. The steady-state multi cycle affinity data were fitted using the Biacore 8K BIAevaluation software.

Single-molecule fluorescence microscopy

- Generation of stable cell lines

HeLa cells, which stably express the IRF4-HaloTag fusion protein were produced by lentiviral transduction (*68*). Briefly, HEK293T cells were transiently transfected with the plasmids psPAX2 (Addgene, USA), pMD2.G (Addgene, USA) and pLV-tetO IRF4-HaloTag using JetPrime (PolyPlus, France) according to the manufacturers protocol. The virus in the supernatant of these cells was harvested through a 0.45 µm filter after 48 h. With this, HeLa cells were infected for 72 h at 37°C and 5% CO2.

- Preparation of cells for imaging

Cells were seeded on a heatable glass bottom Dela T dish (Bioptechs, USA) one day before imaging. Prior to imaging, cells were incubated in 2 pM silicon rhodamine (SiR) HaloTag ligand (kindly provided by Kai Johnson, MPI, Heidelberg, Germany) for 15 min following the HaloTag staining protocol (Promega, Germany). Subsequently, the cells were washed with PBS and recovered for 30 min in DMEM at 37 °C and 5% CO2. For imaging, the cells were washed three times with PBS and imaged in 2 ml OptiMEM.

- Microscope setup

We used a custom-built fluorescence microscope for single-molecular fluorescence imaging (*69*). It was built around a TiE Nikon microscope body and equipped with a 638 nm laser (IBEAM-

SMART-640-S, 150 mW, Toptica), AOTF (AOTFnC-400.650-TN, AA Opto-Elctronic, France) and a high-NA objective (100x, NA 1.45, Nikon). The fluorescence signal passed a multiband emission filter (F72-866, AHF, Germany) and was detected by an EMCCD camera (iXon Ultra DU 897, UK).

- Interlaced time-lapse illumination and data analysis

We illuminated the cells with a highly inclined light beam (*70*) using an interlaced time-lapse illumination scheme (ITM) (*69*). In ITM, we repeated a pattern of two consecutive images with 50 ms camera integration time followed by a dark-time of 2 s. To detect and localize fluorescent molecules within an image and to track molecules across consecutive images we used the analysis software TrackIt v1.0.1 (*71*). Parameters for detection and tracking were: 'threshhold factor' 3, 'tracking radius' 2, 'min. track length' 2, 'gap frames' 0, 'min. track length before gap frame' 0. We classified molecules that were only detected within a single image as unbound, molecules that were detected in two consecutive images within an area of 0.35 μm^2 as short-bound and molecules tracked over at least one dark-time period as long-bound molecules. The ratio of all bound molecules (including short- and long-bound molecules) to all molecules (including long-, short- and unbound molecules) and of long-bound molecules to all molecules was calculated for each imaged cell. Significance between IRF4-WT and IRF4-T95R was tested with an unpaired, non-parametric t-test (Mann-Withney-test) using GraphPad Prism 9.0.1.

Deep learning models

Six different ExplaiNN models, each with 100 units, were trained on either $IRF4^{T95R}$, $IRF4^{WT}$, AICE or EICE ChIP-seq data, or the two *in vitro* datasets (i.e., HT-SELEX). The architecture of each unit was as follows:

- 1st convolutional layer with 1 filter (26x4; 19x4 for training on the HT-SELEX data), batch normalization, exponential activation to improve the representation of the learnt sequence motifs (*72*) and max pooling (7x7);
- 1st fully connected layer with 100 nodes, batch normalization, ReLU activation and 30% dropout; and
- 2nd fully connected layer with 1 node, batch normalization and ReLU activation.

The four models trained on $IRF4^{T95R}$, $IRF4^{WT}$, AICE and EICE ChIP-seq data were further used in a transfer learning strategy to initialize the filter weights of an additional "surrogate" ExplaiNN model with 400 units (100 units x 4 models), which was fine-tuned on $IRF4^{T95R}$ and $IRF4^{WT}$ ChIP-seq data (Fig. S9C). During fine-tuning, filter weights were frozen to prevent them from being refined (i.e., the surrogate model was only allowed to learn the weights of the fully connected and final linear layers).

For training the $IRF4^{T95R}$ and $IRF4^{WT}$ models, ChIP-seq peaks were resized to 201 bp by extending their summits 100 bp in each direction using BEDTools slop (version 2.30.0) (*73*). Negative sequences were obtained by dinucleotide shuffling each dataset using BiasAway (version 3.3.0) (*74*). Sequences were randomly split into training (80%), validation (10%) and test (10%) sets using the "train_test_split" function from scikit-learn (version 0.24.2) (*75*) (datasets were always randomly split in this way).

For training the AICE and EICE models, BATF (ENCFF728KFD), IRF4 (ENCFF113VGD), JUNB (ENCFF912OPT) and PU.1 ChIP-seq data (ENCFF492ZRZ) from GM12878 cells were retrieved from ENCODE (*22*). ChIP-seq peaks were resized to 201 bp, similarly to the $IRF4^{T95R}$ and $IRF4^{WT}$ datasets. AICE peaks were obtained by intersecting the BATF, IRF4 and JUNB peaks using BEDTools intersect. Similarly, EICE peaks were obtained by intersecting IRF4 and PU.1

peaks. In both cases, non-overlapping IRF4 peaks were used as negative sequences, after which sequences were randomly split into training (80%), validation (10%) and test (10%) sets.

For fine-tuning the transfer learning model, $IRF4^{T95R}$ and $IRF4^{WT}$ 201 bp-long ChIP-seq peaks were intersected using BEDTools. Since the number of $IRF4^{T95R}$-specific, $IRF4^{WT}$-specific and intersected (i.e., common) peaks was different, we subsampled them to an equal number while accounting for their %GC content distributions. The resulting sequences were randomly split into training (80%), validation (10%) and test (10%) sets.

For training the HT-SELEX models, each cycle was treated as an independent class as in Asif and Orenstein (*76*), thereby removing the need for negative sequences. Reads were randomly split into training (80%), validation (10%) and test (10%) sets while preserving the proportions between reads from each cycle.

Models were trained as described in ExplaiNN. Briefly, using the Adam optimizer (*77*) and binary cross entropy as loss function, applying one-hot encoding, setting the learning rate to 0.003 (10 times lower for fine-tuning) and batch size to 100, and using an early stopping criteria to prevent overfitting. Models were also interpreted following the specifications from ExplaiNN. The filter of each unit was converted into a motif by aligning al sub-sequences activating that filter's unit by ≥50% of its maximum activation value in correctly predicted sequences. The importance of each motif was calculated as the product of the activation of its unit for each correctly predicted sequence activating that unit by ≥50% of its maximum activation value times the weight of the final layer of that unit for the prediction of $IRF4^{T95R}$-specific, $IRF4^{WT}$-specific, or common ChIP-seq peaks.

Clinical summaries of the patients

Family 1, Patient 1

Patient 1 (P1) was born to healthy, nonconsanguineous parents. He received all pediatric vaccines, including BCG at birth, that were all well tolerated. He was healthy until age of 6 months when he developed his first pneumonia. From the age of 6 months to 3 years, he experienced recurrent upper respiratory tract infections that responded appropriately to antibiotics. From age 3 to 8 years, he was admitted several times for recurrent pneumonias. Pathogens identified in the sputum included *Streptococcus pneumoniae, Haemophilus influenzae, Mycoplasma pneumoniae* and adenovirus. At age 7, he was diagnosed with hypoglobulinemia (IgG 1.96 g/L, IgM 0.08 g/L, IgA 0.02 g/L) and had reduced, but not absent, B cells in peripheral blood (CD19 104/uL). By the age of 8, bronchiectases were revealed by chest CT and IgG replacement therapy was initiated. He also received long-term antimicrobial prophylaxis including amoxicillin-clavulanate, clarithromycin, and fluconazole. Since then, the frequency of respiratory infections was reduced. Gastrointestinal manifestations were also prevalent in P1. He suffered from chronic diarrhea since the age of 3 years, and progressively worsening abdominal pain since age 11 years. Endoscopic examination showed proctocolitis, as well as mucosal eosinophilia (eosinophil count per high power field: 50 in the intestine, 100 in the descending colon, and 110-120 in the rectum). Abdominal CT indicated multiple enlarged lymph nodes in the abdominopelvic cavity and enhanced signal in part of the intestinal mucosa. Treatments with cyproheptadine, omeprazole, acyclovir, and sirolimus seemed to be ineffective, although abdominal pain was partially relieved by prednisone. Since the age of 10 years, P1 developed a non-itchy maculopapular rash on his face, limbs, the back of the hands, and feet. Peripheral blood EBV viral load at that time was positive at 1550 copies/mL. A skin biopsy showed scattered lymphocyte infiltrates around small vessels in the dermis while EBV immunohistochemistry was negative. At age 13 years, P1 received a hematopoietic stem cell transplant (HSCT) from a matched unrelated donor. At the time of this report, 7 months post-HSCT, the patient is fully engrafted with full chimerism and with complete resolution of his enteropathy.

Family 2, Patient 2

Patient 2 (P2) was born to non-consanguineous parents and no family history of immune disorders apart from a maternal history of rheumatoid arthritis. This previously healthy male tolerated all routine immunizations including rotavirus. At 11 months of age, he presented with respiratory failure requiring mechanical ventilation. Rhinovirus/enterovirus, *Pneumocystis jirovecii* pneumonia (PCP), cytomegalovirus (CMV) viremia and *Escherichia coli* ventilator-associated pneumonia ensued. The patient's infections were treated and resolved with standard antimicrobial therapies. He was maintained on a regimen of monthly intravenous IgG replacement therapy together with prophylactic cotrimoxazole and valganciclovir.

Initial immunological assessment was noteworthy for agammaglobulinemia (IgG <0.3 g/L, IgA < 0.04 g/L and IgM < 0.03 g/L), undetectable titers to tetanus and diphtheria toxoids and reduced lymphocyte proliferation stimulation index (SI) to phytohemagglutinin with a normal response to pokeweed mitogen. The presence of lymphocytes including peripheral T and B lymphocytes was confirmed (x 10e9 cells/L): CD3 cells 3.74, CD4 cells 2.82, CD19 cells 1.14, NK cells 0.04 (all normal for age). Normal T cell memory subsets. B cell memory subsets demonstrated a low proportion of class switched memory B cells and borderline increase in naïve B cells.

At the age of 2 years the patient received his first HSCT from a matched unrelated donor. HSCT was complicated by loss of donor graft three times due to ongoing multi-drug resistant CMV infection, CMV end-organ disease and *Aspergillus* lung infection. P2 is currently fully engrafted

with a CMV viral load of zero following a fourth HSCT from a haploidentical donor although follow-up time is only 6 months at the time of writing.

Family 3, Patient 3

Patient 3 (P3) was born to healthy, non-consanguineous parents. The patient presented in the first month of life with bronchiolitis and recurrent respiratory tract infections. He had diarrhea with documented rotavirus infection at 1.5 month of age and developed failure to thrive requiring supplemental enteral feeding. At the age of 6 months, he suffered from PCP, norovirus, enterovirus, and rhinovirus infection. Immunological investigations revealed agammaglobulinemia while B lymphocytes were present in the blood. Since then, he has been on immunoglobulin replacement therapy and cotrimoxazole prophylaxis. The percentage of memory B cells ($CD19^+CD27^+$) was always below reference values. IgA levels were undetectable (<0.03 g/L) until the age of 4 years when they were found at 0.14 g/L, and levels remained low (0.15 g/L at 8 years, 0.40 g/L at 9 years 10 months, respectively). However, IgM serum level remained undetectable (<0.05 g/L). T cell $CD8^+$ naïve cells were increased in frequencies in contrast to CD8+ effector memory and $CD8^+$ terminal effector memory RA+ cells, which were below age matched values. The patient height and weight caught up after his initial failure to thrive and had normal development during childhood. He was well and attending regular school without significant health problems until the age of 9.5 years at which he suffered from a second episode of PCP infection due to poor adherence to cotrimoxazole prophylaxis.

Family 4, Patient 4

Patient 4 (P4) is a five-year-old boy born to non-consanguineous parents. He was born at term and remained healthy until he turned 6 months old, when he was admitted at the pediatric intensive care unit with a suspected PCP. Since then, he has had recurrent respiratory infections of unknown etiology, some of which required hospitalization. At the age of 15 months, he presented with prolonged diarrhea (non-responsive to antibiotics) that was accompanied by a 2.5kg weight loss. When he was 2y, he developed a localized regional BCGitis which responded to isoniazid, rifampicin, pyrazinamide, and ethambutol treatment. Immunologically, he showed reduced levels of circulating immunoglobulins (IgG 1.69 g/L, IgA 0.06 g/L, IgM 0.09 g/L) consistent with a diagnosis of hypogammaglobulinemia. Since the age of 2 years, he has been on prophylactic treatment with fluconazole, cotrimoxazole, and IgG replacement therapy. At the age of 5 years, he received a HSCT from his haploidentical mother (1-month post-HSCT at the time of manuscript submission).

Family 5, Patient 5

Patient 5 (P5) is a male patient who was born to non-consanguineous parents. He presented at the age of 4 months with recurrent respiratory infections; at the age of 7 months, he was admitted with a positive *Pneumocystis jirovecii* and CMV respiratory infection. With absent serum levels for IgG, IgM and IgA, absent specific antibodies for tetanus toxoid and *Haemophilus influenzae Type B* (after three vaccinations), a combined immunodeficiency was suspected. He recovered well on an anti-infectious regimen containing cotrimoxazole and ganciclovir. Immunophenotyping revealed normal counts for T, B and NK cells with a normal proportion of naïve CD4 positive cells. T-cell function after non-specific (PHA, anti-CD3/-CD28) and specific (tetanus toxoid, mixed lymphocyte culture) stimulation was found positive, but resulted negative against CMV. The patient was placed on IgG replacement therapy and cotrimoxazole prophylaxis. At the age of 20 months (7 months after cotrimoxazole discontinuation) he experienced a second *Pneumocystis jirovecii* pneumonia which required mechanical ventilation. He recovered with therapeutic

cotrimoxazole and remained on pneumocystis prophylaxis since then. Extensive onychomycosis involving his finger- and toenails has been persistent since the age of 3 years. In the next 20 years of follow up, no other serious infectious complications occurred, whilst the patient continued prophylaxis and he did not develop any relevant complications or organ damage.

Family 6, Patient 6 and Patient 7

Patient 6 (P6) and Patient 7 (P7) were born to healthy, non-consanguineous Argentine parents. Both patients received all pediatric vaccines, including BCG at birth, that were well tolerated.

P6, the elder sister, was healthy until the age of 5 months when she started experiencing recurrent episodes of hypoxia, several of them requiring hospitalization. At age 6 month she was admitted with pneumonitis, suspected to be due to *Pneumocystis jirovecii* (no bronchoalveolar lavage or specific stains were performed, rapid response to cotrimoxazole was achieved). At age 1 year she who diagnosed with agammaglobulinemia (IgG: 0.10 g/L; IgA and IgM: not detectable) with B cells present in peripheral blood (CD19 3293/uL; 28% of total lymphocytes). Since early childhood she also presented with repeated upper sinopulmonary infections including suppurative otitis media, adenoiditis, sinusitis and oto-mastoiditis; the latter complicated with lateral sinus thrombosis for which she needed prolonged anticoagulation. Due to severe adenoid hypertrophy, at age 8 years an adenoidectomy was performed, and bilateral tympanostomy tubes were placed. She is currently on IgG replacement therapy and cotrimoxazole prophylaxis.

P7, 5 years younger than his sister P6, was also healthy until the age of 5 months when he started experiencing recurrent episodes of bronchospasms. At the age of 7 months, he was admitted with *Pneumocystis jirovecii* pneumonia, which responded adequately to cotrimoxazole therapy. During this admission he was diagnosed with agammaglobulinemia (IgG: 0.24 g/L; IgA: 0.02 g/L; IgM: 0.03 g/L) with reduced but present B cells in peripheral blood (CD19 463/uL; 7.7% of total lymphocytes). Due to severe tonsil hypertrophy, the patient had a tonsillectomy at age 4 years; soon after, a fast growing left cervical lymph node was also excised. The left tonsil and the left lymph node showed multiple acid-fast bacilli and granuloma formation by histopathologic analysis. The organism cultured from the lymph node was characterized as *Mycobacterium bovis*. Besides his IgG replacement therapy and cotrimoxazole, the mycobacterial infection is currently being treated with isoniazid, rifampin, and clarithromycin.

Supplemental Figure 1 (related to Figure 1)

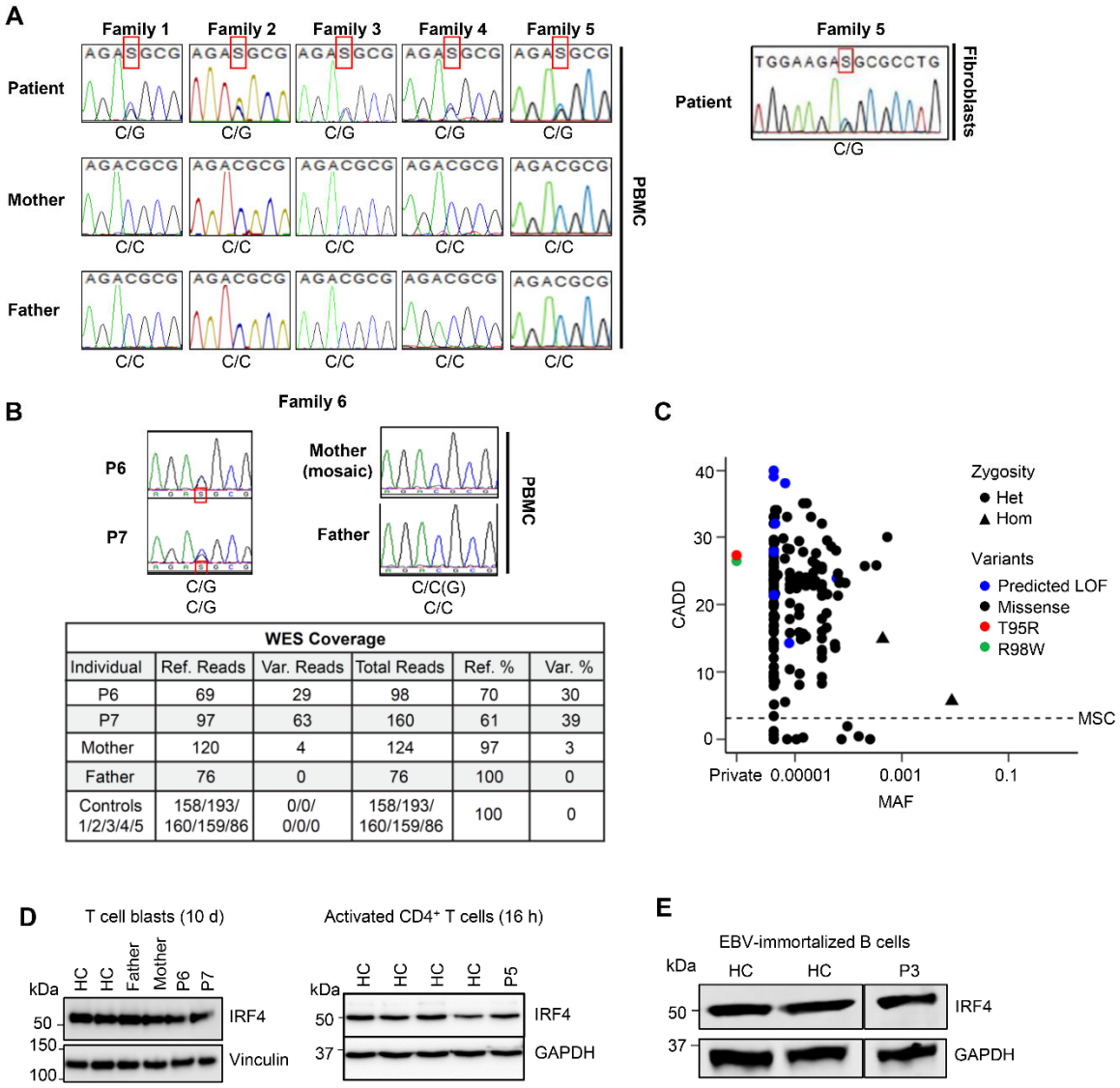

WES Coverage					
Individual	Ref. Reads	Var. Reads	Total Reads	Ref. %	Var. %
P6	69	29	98	70	30
P7	97	63	160	61	39
Mother	120	4	124	97	3
Father	76	0	76	100	0
Controls 1/2/3/4/5	158/193/ 160/159/86	0/0/ 0/0/0	158/193/ 160/159/86	100	0

Fig. S1. Identification of a unique heterozygous mutation in the *IRF4* gene in seven CID patients. (**A**) Sanger sequencing of *IRF4* genomic DNA from PBMC of families 1-5 (left) and from fibroblasts of P5 (right). (**B**) Upper, Sanger sequencing of PBMC from P6, P7 and their parents. The mother appeared to carry a mosaic mutation. Below, Whole-exome sequencing (WES) from DNA obtained from peripheral blood revealed that 4 out of 124 sequences from the mother were mutated. (**C**) Minor allele frequency (MAF) and combined annotation-dependent depletion (CADD) score of all coding and essential splicing variants of IRF4. (**D**) Left, PBMC from P6 and P7, their parents and two HC were stimulated with anti-CD3/CD28 beads in the presence of IL2 for 10 days, and analyzed for IRF4 protein expression by immunoblot. Vinculin was used as a loading control; Right, $CD4^+$ T cells purified from P5 and 4 HC were stimulated with anti-CD3/CD28 beads for 16 h and analyzed for IRF4 expression by immunoblot. GAPDH was used as a loading control. (**E**) IRF4 protein levels in EBV-immortalized B cell lines from P3 and two HC. GAPDH was used as a loading control.

Supplemental Figure 2 (related to Figure 2)

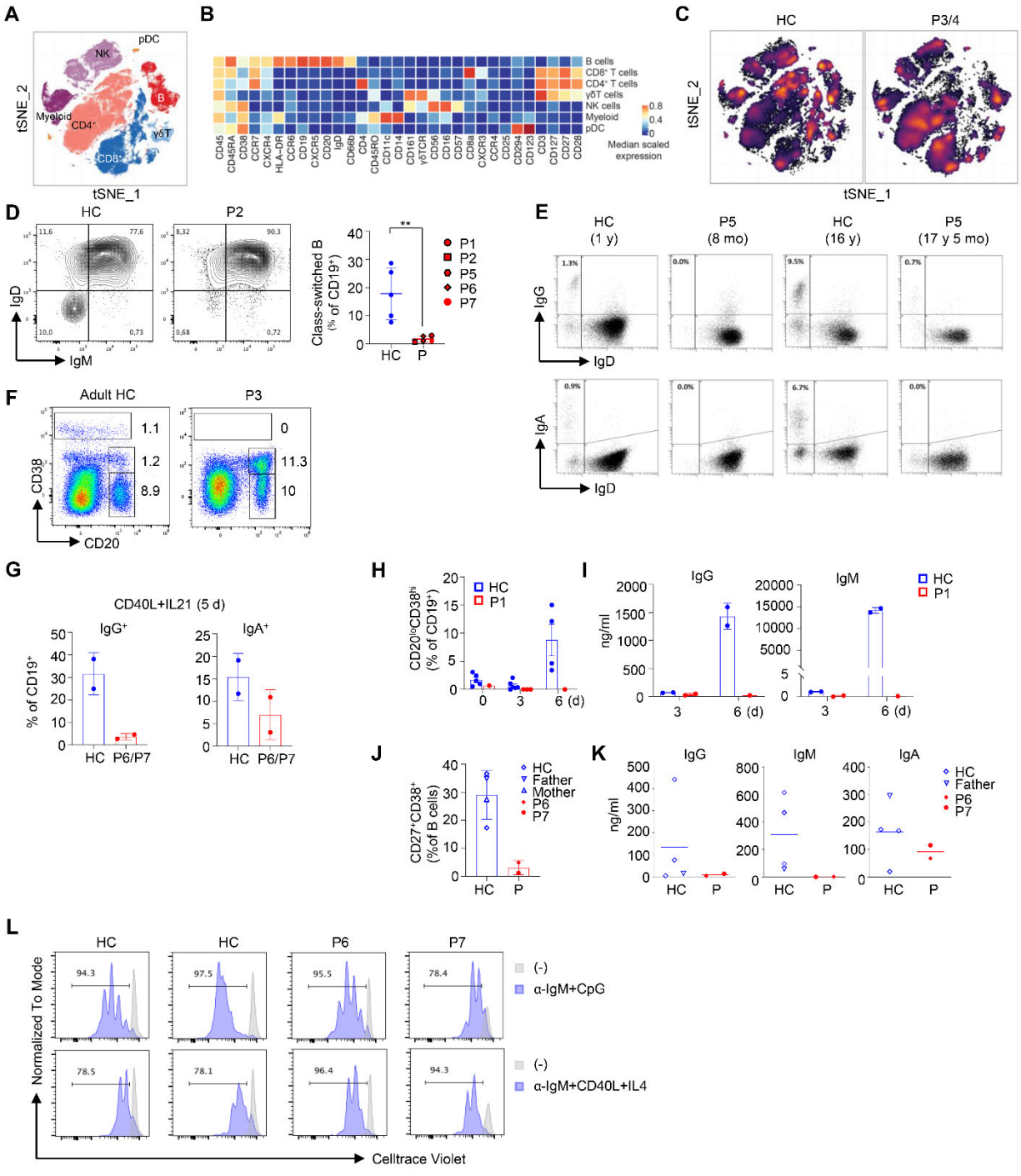

Fig. S2. Overt immunological phenotype, impaired Ig gene CSR and defective PC differentiation in IRF4^{T95R} patients. (A-C) CyTOF analysis of PBMC from P3, P4 and 5 healthy controls. **(A)** Dimensional reduction by t-SNE of the 31 markers used for immunophenotyping by mass cytometry. Each color represents a cell population obtained by manual clustering according to their surface marker expression. (**B**) Heatmap showing marker expression of the populations in Fig. S2A. (**C**) Density tSNE showing comparing cell distribution among and within the populations shown in Fig. S2A. (**D**) Left, representative flow cytometric profiles showing the IgM$^-$ IgD$^-$ class-switched B cells in gated CD19$^+$ cells; Right, summary of the data from P1, P2 and P5-P7 and their age-matched HC. (**E**) Frequencies of class-switched (IgG$^+$IgD$^-$ or IgA$^+$IgD$^-$) cells among CD19$^+$ B cells in PBMC from P5 (at ages of 8 m and 17 y 5 m) and two HC (1 y and 16 y). (**F**) CD38^{hi} plasmablasts were barely detectable in the BM of P3 compared with an adult HC. (**G**) PBMC of P6 and P7 and two HC were stimulated with CD40L + IL21 for 5 days. Percentages of IgG$^+$ and IgA$^+$ cells among CD19$^+$ B cells are shown. Data represent mean ± S.D. (**H**) PBMC of six HC and P1 were cultured with CMIL2 for three and six days and analyzed for PC differentiation. (**I**) IgG and IgM levels in the culture supernatants of Fig. S2H. (**J**) PBMC of two HC, P6 and P7 and their parents were cultured with CD40L + IL21 for four days and analyzed for PC differentiation. Data represent mean ± S.D. (**K**) Naïve B cells were stimulated with CD40L and IL21 for 6 days. IgG, IgM and IgA levels in the culture supernatants were measured. The horizontal lines indicate mean values. (**L**) Total PBMCs from P6 and P7 and two HC were cultured with the indicated stimuli for 4 days and B-cell proliferation was assessed by celltrace violet dilution. $^{**}p < 0.01$.

Supplemental Figure 3 (related to Figure 3)

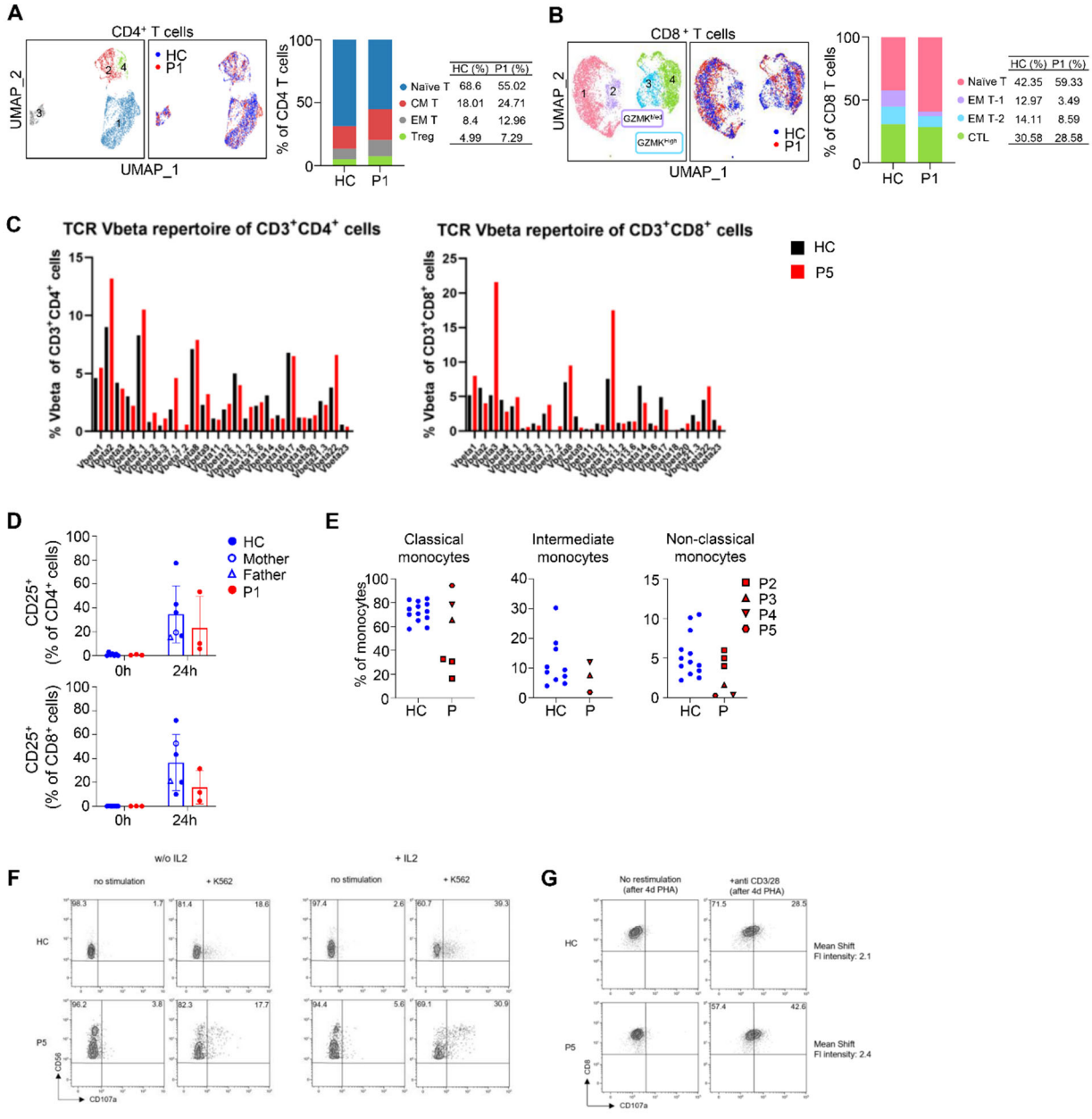

Fig. S3. Altered T cell differentiation and function in IRF4^{T95R} patients. (**A** and **B**) scRNA-seq of peripheral T cells from P1. (**A**) Left, UMAP profiles of CD4$^+$ T cells; Right, frequencies of naïve, CM, EM and Treg subsets among CD4$^+$ cells. (**B**) Left, UMAP profiles of CD8$^+$ T cells; Right, frequencies of naïve, EM T-1, EM T-2 and CTL subsets among CD8$^+$ cells. (**C**) TCR Vβ repertoire in CD3$^+$CD4$^+$ (left) and CD3$^+$CD8$^+$ (right) T cells of P5 and HC. (**D**) CD25 expression in CD4$^+$ (upper) and CD8$^+$ (lower) T cells of HC and P1 before (0 h) and after (24 h) stimulation with anti-CD3 + anti-CD28. (**E**) Proportions of classical (left), intermediate (middle) and non-classical monocytes among total monocytes in PBMC of P2- P5 (Supplemental Table 11). (**F**) NK-cell degranulation assay using NK cells from P5 PBMC as effector cells and K562 cells as target cells. Assays were performed without IL2 and with IL2. FACS profiles showing CD107A release by NK cells. (**G**) CD8$^+$ T cells from HC and P5 were stimulated with PHA for 4 days and then re-stimulated with anti-CD3/anti-CD28, and analyzed for CD107a expression (degranulation).

Supplemental Figure 4 CD4 T (related to Figure 3)

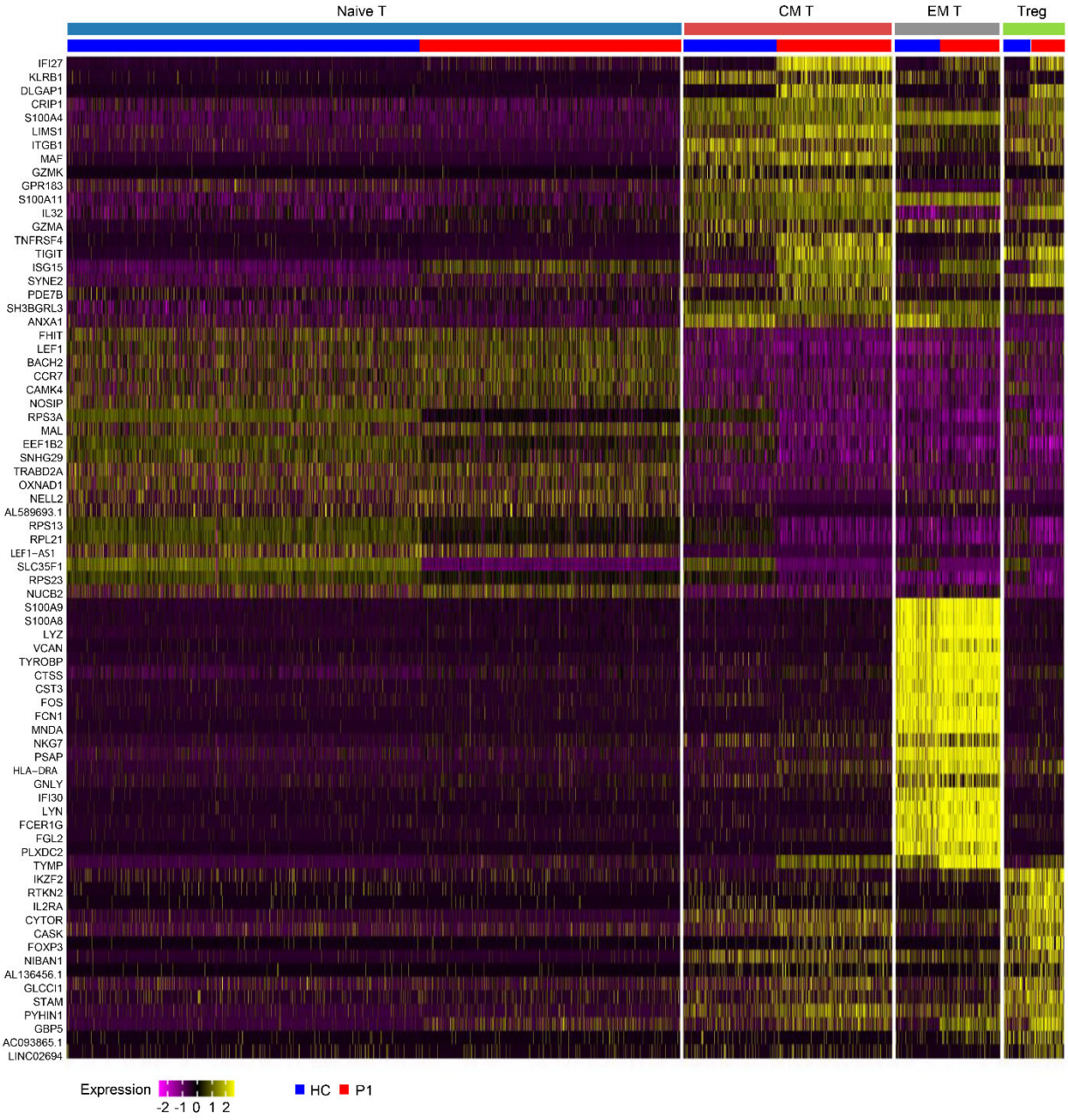

Fig. S4. Heat map of Top 20 differentially expressed (DE) genes in the four CD4 T cell clusters, colored as in Fig. S3A.

Supplemental Figure 5 CD8 T (related to Figure 3)

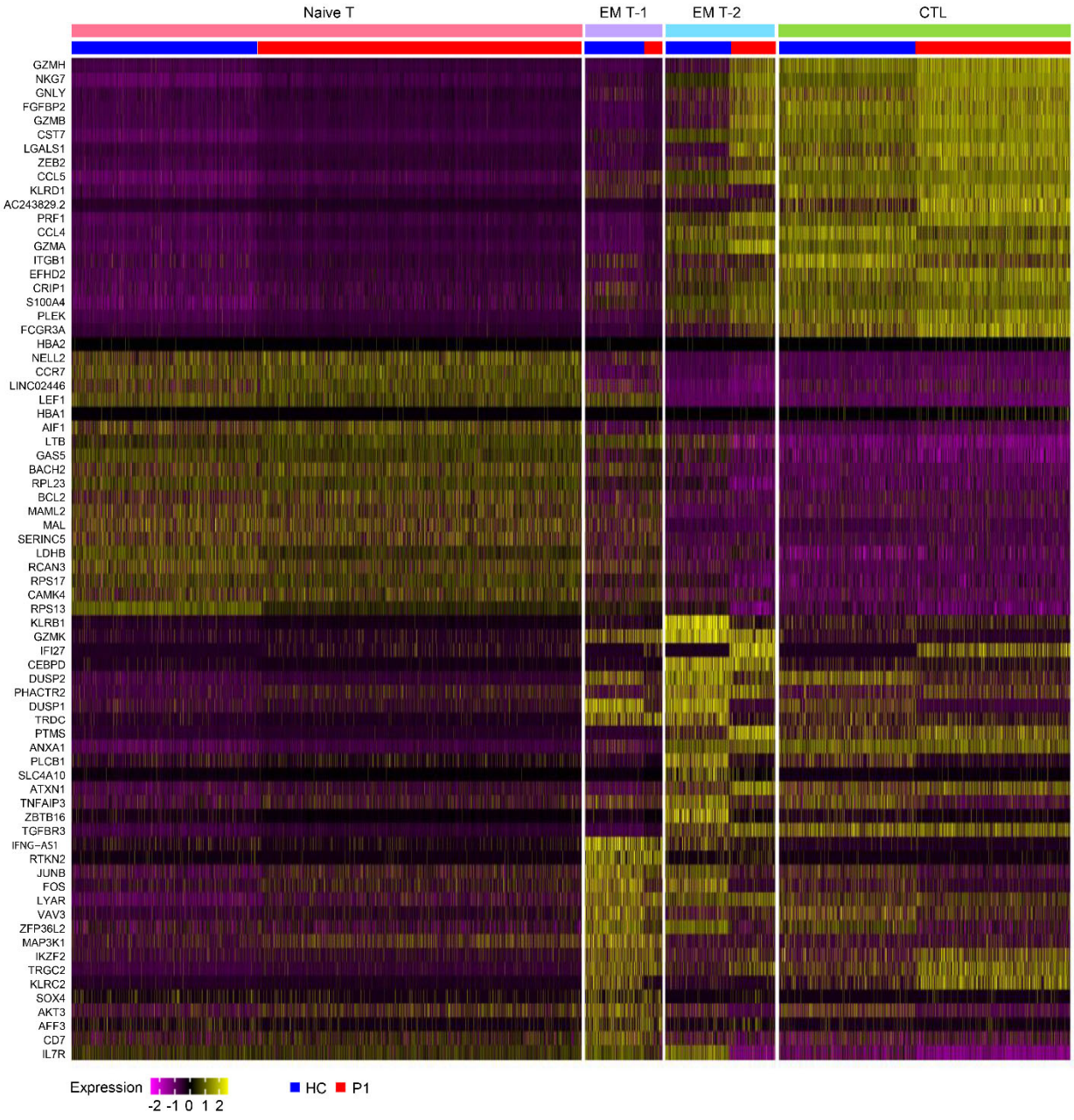

Fig. S5. Heat map of Top 20 DE genes in the four CD8 T cell clusters, colored as in Fig. S3B.

Supplemental Figure 6 (related to Figure 4)

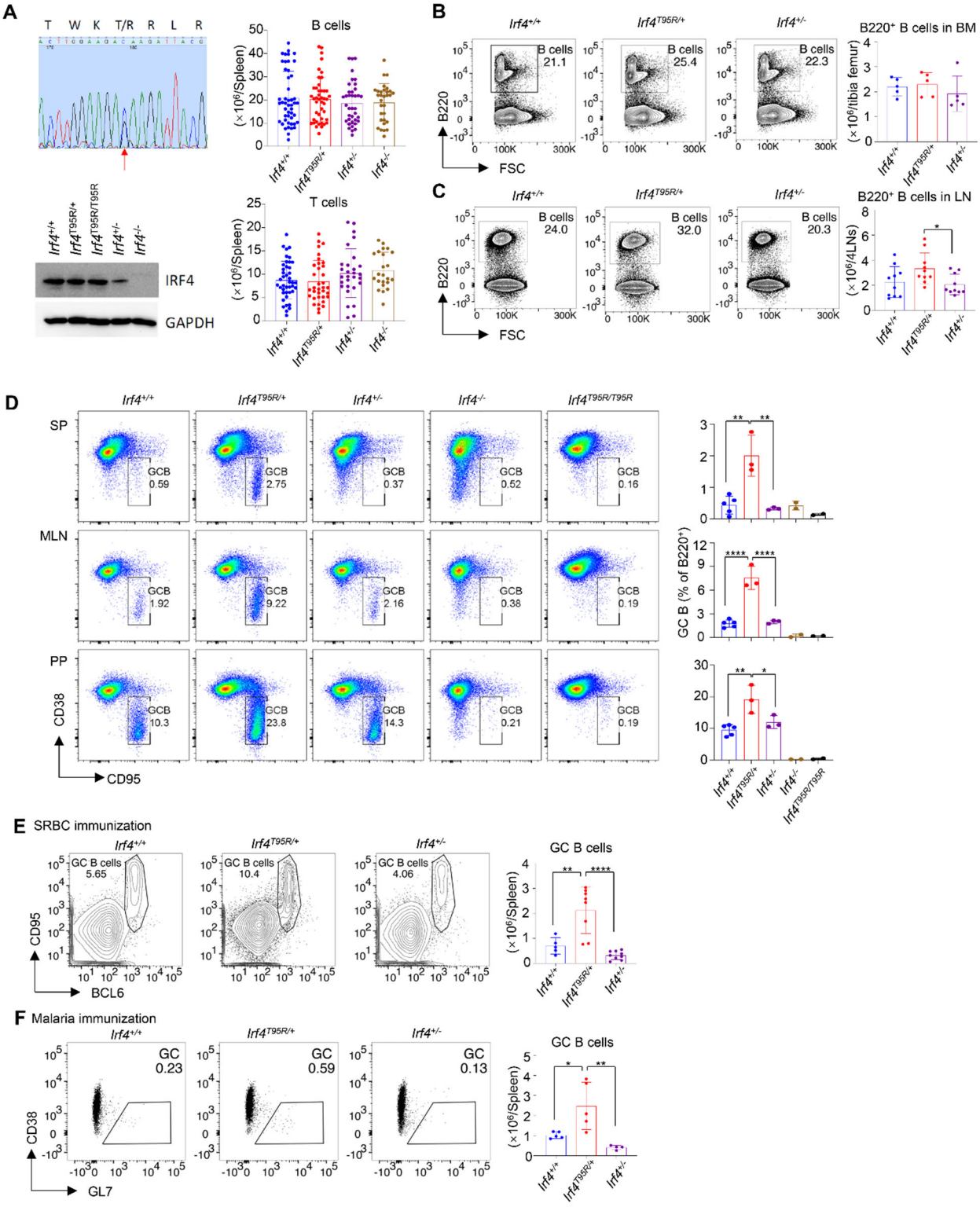

Fig. S6. Spontaneous GC B-cell expansion but defective antibody production in *Irf4*$^{T95R/+}$ mice. (**A**) Upper left, sequencing profile of the founder mouse generated in ANU. Lower left, an IRF4 immunoblot using spleen B cells purified from different genotypes. Number of B (upper right) and T (lower right) cells in the spleen of WT and mutant mice. (**B**) Representative proportions and summary of numbers of $B220^+$ cells in the BM. (**C**) Representative proportions and summary of numbers of $B220^+$ cells in the LN. (**D**) Percentages of the $CD38^-CD95^+$ GC B cells among $B220^+$ cells in the spleen (SP), mesenteric lymph nodes (MLN) and Peyer's patches (PP) of *Irf4*$^{+/+}$, *Irf4*$^{T95R/+}$, *Irf4*$^{+/-}$ *Irf4*$^{-/-}$ and *Irf4*$^{T95R/T95R}$ mice. Left, representative flow cytometric profiles; Right, summary data. (**E**) Representative proportions and summary of numbers of $BCL6^+CD95^+$ GC B cells among $B220^+$ cells in the spleen after SRBC immunization. (**F**) Representative proportions and summary of numbers of $GL7^+CD38^-$ GC B cells among $B220^+$ cells in the spleen after immunization with irradiated *Plasmodium* sporozoites. *$p < 0.05$; **$p < 0.01$; ****$p < 0.0001$.

Supplemental Figure 7 (related to Figure 4)

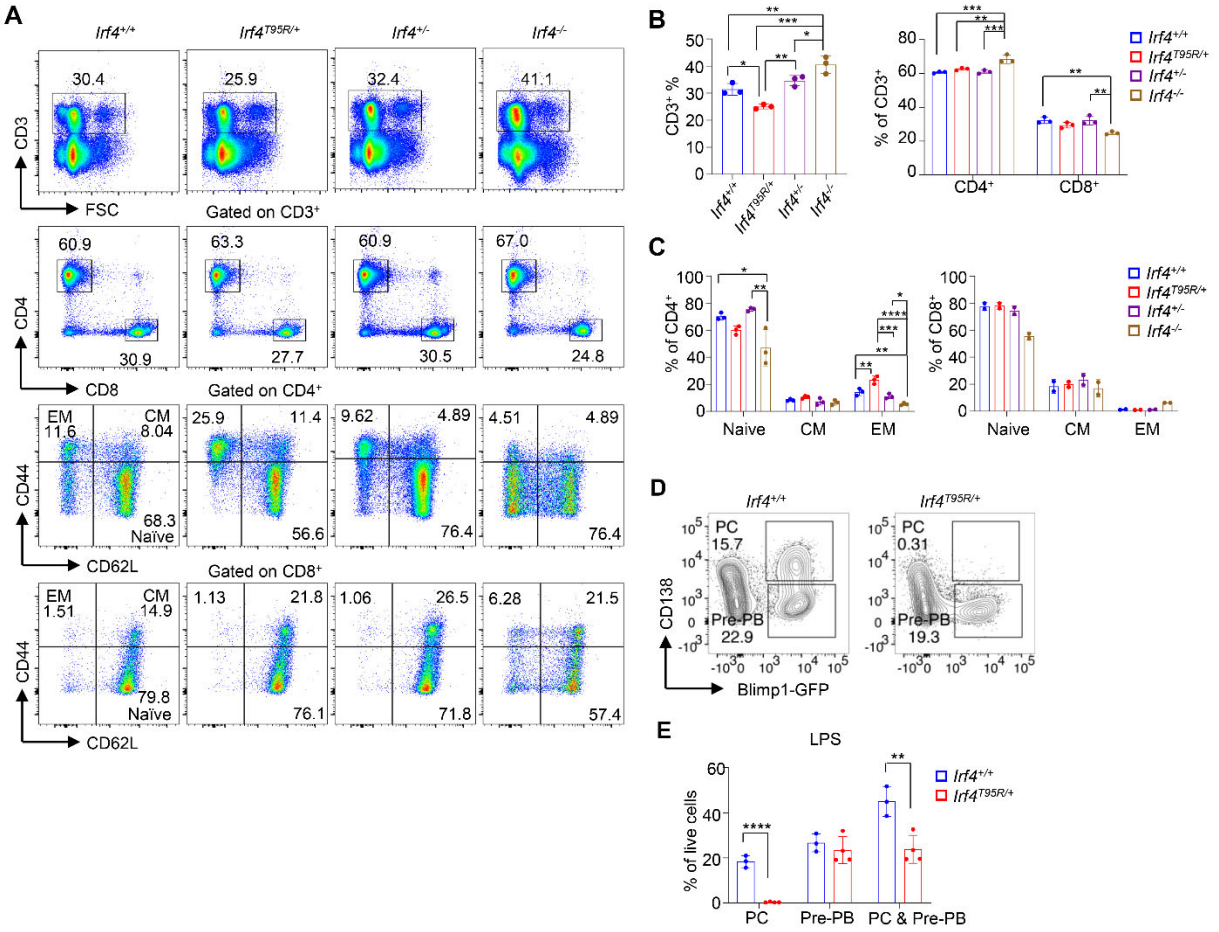

Fig. S7. T-cell subset distribution in the spleen of *Irf4*$^{+/+}$, *Irf4*$^{T95R/+}$, *Irf4*$^{+/-}$ and *Irf4*$^{-/-}$ mice. (**A**) From top to bottom, representative flow cytometric profiles of CD3 vs. FSC, CD4 vs. CD8 in gated CD3$^+$ cells, and CD44 vs. CD62L in gated CD4$^+$ or CD8$^+$ T cells. (**B**) Percentages of CD3$^+$ T cells (left) among live cells and CD4$^+$ and CD8$^+$ T cells among CD3$^+$ cells (right). (**C**) Proportions of naïve (CD62L$^+$CD44$^-$), CM (CD62L$^+$CD44$^+$) and EM (CD62L$^-$CD44$^+$) T cells among total CD4$^+$ (left) and CD8$^+$ (right) cells. (**D**) Spleen B cells purified from WT or *Irf4*$^{T95R/+}$ Blimp1-GFP reporter mice were cultured for 3 days in the presence of LPS and analyzed for the induction of GFP and CD138 expression. *Irf4*$^{T95R/+}$ B cells were able to activate Blimp1 transcription but failed to upregulate CD138 expression. (**E**) Summary of 3 independent experiments shown in Fig. S7D. Data are presented as mean ± S.D. *$p < 0.05$; **$p < 0.01$; ***$p < 0.001$; ****$p < 0.0001$.

Supplemental Fig 8 (related to Figure 5)

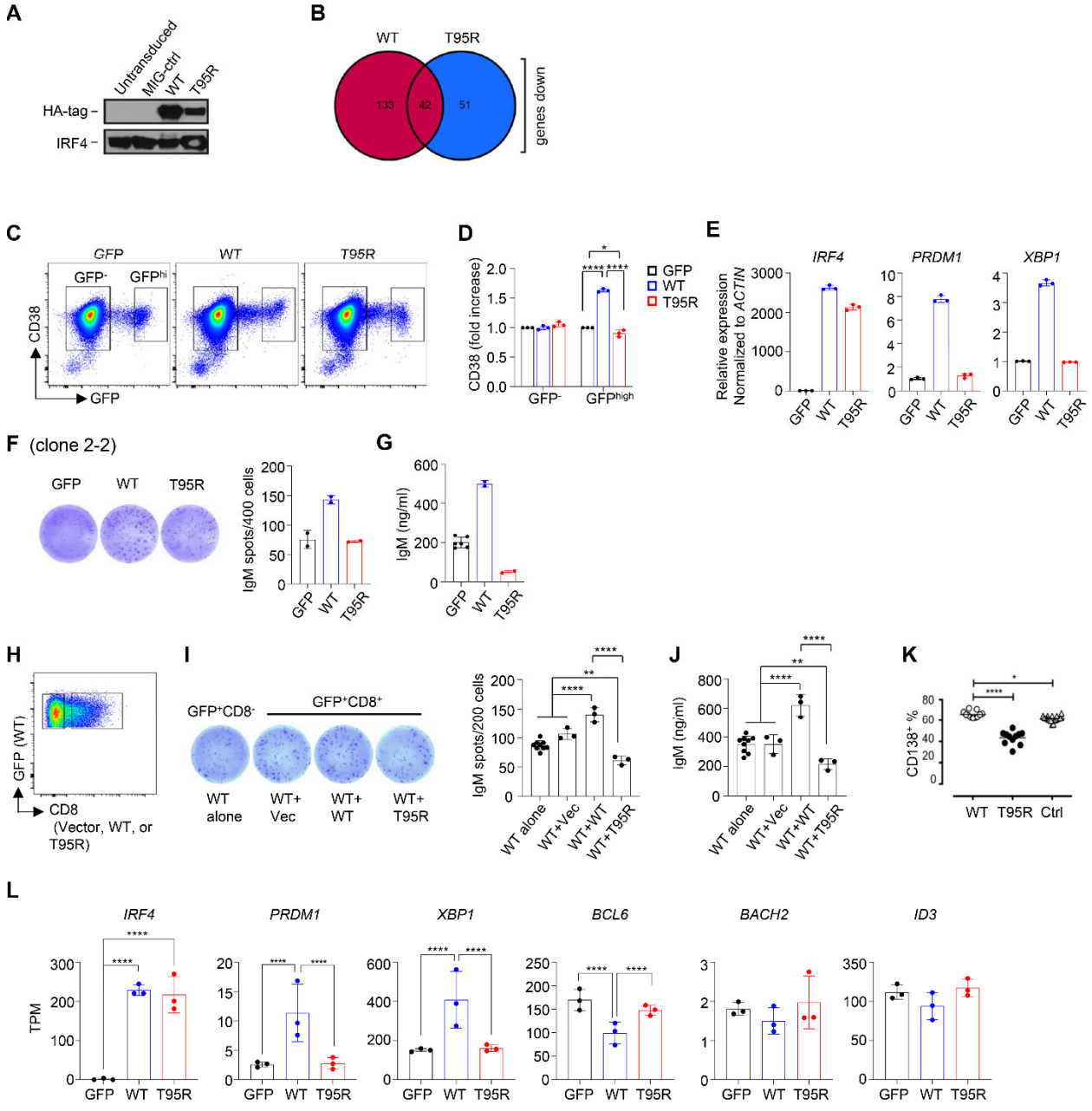

Fig. S8. IRF4^{T95R} was unable to induce PC differentiation due to the inability to activate the expression of genes involved in the PC differentiation program. (A) Mouse C75BL/6 splenic B cells were cultured with LPS+IL4, transduced with control retrovirus (MIG-ctrl), IRF4^{WT} or IRF4^{T95R}, or not transduced, and analyzed for protein levels of IRF4 by western blot using an antibody against HAtag for detection of ectopically expressed IRF4, or an antibody to IRF4 for detection of IRF4 overall protein levels. **(B)** Genes differentially downregulated by IRF4^{WT}, and IRF4^{T95R} show limited overlap. (**C** and **D**) Raji cells were transduced with retrovirus expressing GFP alone, IRF4^{WT} or IRF4^{T95R} and analyzed for CD38 expression in gated GFP^{-} or GFP^{high} cells 3 days later. (**C**) Representative FACS profiles showing the gate for GFP^{-} and GFP^{high} cells. (**D**) CD38 level in Raji cells expressing IRF4^{WT} or IRF4^{T95R}, relative to that in Raji cells expressing GFP alone, which was set to 1. Mean ± S.D. of 3 independent experiments is shown. (**E**) Raji cells were transduced with retrovirus as in Fig. S8C and analyzed for *IRF4*, *PRDM1* and *XBP1* expression in sorted GFP^{+} cells by real-time PCR. The value in Raji cells expressing GFP alone was set to 1. Representative results of 3 independent experiments are shown. (**F** and **G**) IRF4-deficient Ramos cells (clone 2-2) were transduced with retrovirus expressing GFP alone, IRF4^{WT} or IRF4^{T95R}. The GFP^{+} cells were sorted 3 days later and analyzed for IgM-secreting cells by ELISPOT. (**F**) Left, representative images; right, mean ± S.D. of duplicate wells. (**G**) The sorted cells were further cultured for 5 days and analyzed by for IgM levels in the culture supernatant by ELISA. Mean ± S.D. is shown. (**H-J**) IRF4-deficient Ramos cells were transduced with retrovirus expressing IRF4^{WT}-IRES-GFP together with retrovirus expressing IRF4^{WT}-IRES-CD8, IRF4^{T95R}-IRES-CD8 or an empty vector (**H**) and 3 days later GFP^{+}CD8^{-} and GFP^{+}CD8^{+} cells were sorted for the analyses of antibody-secreting cells by ELISPOT (**I**) and antibody secretion after 5 days' culture (**J**). (**K**) B cells were purified from tonsils of a HC by magnetic cell sorting, activated in vitro with CD40L and IL21 and transduced by lentivirus expressing WT IRF4 or T95R. After 6 days, cells were analyzed for CD138 expression. (**L**) Raji cells were transduced with retrovirus expressing GPF alone, IRF4^{WT} or IRF4^{T95R} and analyzed for the expression (Transcripts Per Kilobase Million, TPM) of *IRF4*, *PRDM1*, *XBP1*, *BCL6*, *BACH2* and *ID3* by RNA-Seq. *$p < 0.05$; **$p < 0.01$; ***$p < 0.001$; ****$p < 0.0001$.

Supplemental Figure 9 (related to Figure 6)

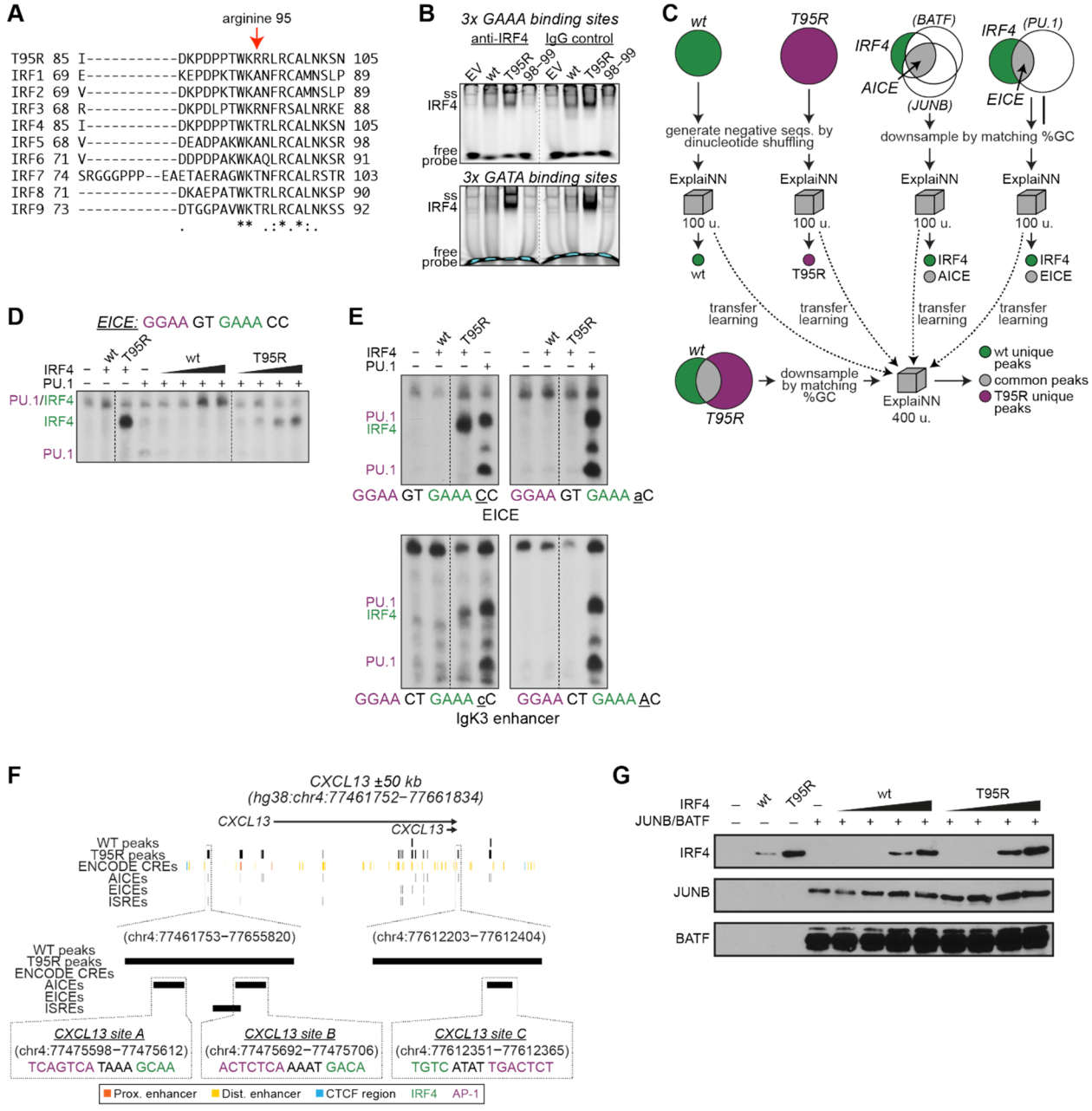

Fig. S9. IRF4^{T95R} showed increased affinity for DNA, altered specificity, and a different IRF4-binding landscape. (**A**) Partial multiple sequence alignment of the nine human IRF proteins and IRF4^{T95R}. (**B**) EMSA showing that IRF4^{T95R} bound to ISRE containing 3x GAAA sites more strongly than did IRF4^{WT} (upper) but also bound to a mutant ISRE with 3x GATA sites (lower). (**C**) Transfer learning strategy used in this work: pre-training four individual ExplaiNN models on IRF4^{WT}, IRF4^{T95R}, AICE or EICE ChIP-seq data, and fine-tuning a multi-task ExplaiNN model on IRF4^{WT}-specific, IRF4^{T95R}-specific, and common ChIP-seq data, previously initialized with the weights of the pre-trained models. (**D**) IRF4^{T95R} alone was able to bind to an EICE but failed to cooperate with PU.1. HEK293 cells were transfected with PU.1 with or without IRF4^{WT} or IRF4^{T95R}, as indicated. Nuclear extracts were analyzed for binding to an EICE site, as indicated. Dashed lines indicate cuts of the scan for presentation. (**E**) HEK293 cells were transfected with PU.1, IRF4^{WT} or IRF4^{T95R}, as indicated. Nuclear extracts were analyzed for binding to two different EICE sites (named EICE and IgK3 enhancer). Note, that increased binding affinity of IRF4^{T95R} depends on a C present in position +1 relative to the GAAA binding motif (present in wildtype configuration of probe EICE, indicated by capital, whereas the IgK3 enhancer probe contains an A in wildtype configuration at +1). Dashed lines indicate cuts of the scan for presentation. (**F**) Schematic overview of the genomic region encompassing the longest *CXCL13* transcript ±50 kb. The presence of IRF4^{WT} and IRF4^{T95R} peaks, as well as ENCODE *cis*-regulatory elements (CREs) and predicted AICE, EICE and ISRE sites in the region is shown. The two IRF4^{T95R} IRF4 ChIP-seq peaks encompassing the CXCL13 sites A, B and C are highlighted. (**G**). Detection of IRF4, JUNB and BATF protein by western blotting in nuclear extracts used for EMSA analyses in panel J of Figure 6.

Table S1. Clinical features of the patients

	P1	P2	P3	P4
Sex	Male	Male	Male	Male
Age	12y	12m	9y10m	4y8m
Age of onset	6m	11m	1m	6m
Clinical symptoms	Recurrent respiratory infections Chronic diarrhea	Recurrent respiratory infections	Recurrent respiratory infections Diarrhea	Recurrent respiratory infections Chronic diarrhea
Respiratory tract/lung	Sinusitis Bronchiectasis	Respiratory failure	Bronchiolitis	Bronchospasms
Skin	Limb rash			
Lymphadenopathy	+			+
Hepatosplenomegaly	+			
Intestinal tract	Mild colitis			
Others	Liver dysfunction			
Infections	*Streptococcus pneumoniae* *Haemophilus influenzae* Salmonella Enterovirus EBV Candida albicans	*Pneumocystis jirovecii* Enterovirus Rhinovirus CMV	*Pneumocystis jirovecii* (2x) Enterovirus Rhinovirus Norovirus Rotavirus	*Pneumocystis jirovecii* suspected BCGitis
Treatment	Antibiotics, IgG replacement HSCT	Antibiotics IgG replacement HSCT (4x)	Antibiotics IgG replacement	Antibiotics IgG replacement HSCT

	P5	P6	P7
Sex	Male	Female	Male
Age	22y	8y	3y
Age of onset	4m	6m	6m
Clinical symptoms	Recurrent respiratory infections	Recurrent infections	Recurrent bronchospasms
Respiratory tract/lung			Bronchospasms
Skin	Onychomycosis		
Lymphadenopathy			
Hepatosplenomegaly			
Intestinal tract			
Others			
Infections	*Pneumocystis jirovecii* (2x) CMV	*Pneumocystis jirovecii* suspected	*Pneumocystis jirovecii* *Mycobacterium bovis*
Treatment	Antibiotics Antimycotics Pneumocystis prophylaxis IgG replacement	Pneumocystis prophylaxis IgG replacement	Antibiotics Pneumocystis prophylaxis, IgG replacement

EBV, Epstein-Barr virus. CMV, cytomegalovirus. HSCT, hematopoietic stem cell transplantation

Table S2. Features of the IRF4 T95R mutation

Variant Annotation	
Chromosome	6
Genomic Position (GRCh38)	394888
cDNA Position (NM_001195286.2)	284
Nucleotide Reference	C
Nucleotide variant	G
Protein Variant (NP_001182215.1)	Thr95Arg; T95R
Zygosity	Heterozygous
Inheritance	P1, P2, P3, P4, P5: de novo P6, P7: maternal mosaic
dbSNP153	No entry
gnomAD (v3.1.1)	No entry
COSMIC (v95)	Somatic report, 2 entries (Mutation ID COSV66704481)
***In silico* Pathogenicity Prediction Models**	
CADD (v1.6)	27.3
SIFT	Deleterious (0)
Polyphen-2	Probably damaging (1)
LRT	Deleterious (0)
MutationTaster	Disease causing (1)
PROVEAN	Deleterious (-5.64)
MetaSVM	Deleterious (1.04)
M-Cap	Possibly pathogenic (0.40)
fathmm_MKL-coding	Deleterious (0.96)

Table S3. Immunological features of patient 1

	8y	Reference value	9y	Reference value	10y	Reference value	12y	Reference value
Serum Abs								
IgG (g/L)	**1.96**	6.09-12.85	**1.24**	6.09-12.85	11.8*	6.09-12.85	13.1*	6.98-14.26
IgA (g/L)	**0.02**	0.52-2.16	**UD**	0.52-2.16	**0.36**	0.52-2.16	**UD**	0.92-2.50
IgM (g/L)	**0.08**	0.67-2.01	**0.08**	0.67-2.01	**0.31**	0.67-2.01	0.599	0.56-2.16
IgE (kU/L)	UD	<100		<100	18.14	<100	UD	<100
B lymphocytes								
$CD19^+$ (/µl)					**104**	200-600	**55**	200-600
$CD19^+$ (%)			**5.72**	9.19-19.48	**6.02**	9.19-19.48	**2.78**	9.19-19.48
Naïve B (% of $CD19^+$) (IgD^+CD27^-)					**89.6**	51.84-77.61	**92.66**	51.84-77.61
Memory B (% of $CD19^+$) (IgD^-CD27^+)					**1.19**	8.96-24.09	**0.19**	8.96-24.09
MZB-Like (% of $CD19^+$) (IgD^+CD27^+)					2.12		1	
Transitional B (% of $CD19^+$) ($CD24^{hi}CD38^{hi}$)					**60.5**	2.50-9.07	**37.95**	2.50-9.07
T lymphocytes								
$CD3^+$ (/µl)					1177	1100-2200	1521	1100-2200
$CD3^+$ (%)			**83.52**	57.10-73.43	63.9	57.10-73.43	**76.97**	57.10-73.43
$CD4^+$ (/µl)					**359**	600-1600	**344**	600-1600
$CD4^+$ (% of $CD3^+$)			18.82	24.00-38.72	31.6	24.00-38.72	**17.43**	24.00-38.72
CD4 naïve T (% of $CD4^+$) ($CD45RA^+CD27^+$)					57.4	39.72-69.59	55.45	39.72-69.59
CD4 central memory T (% of $CD4^+$) ($CD45RA^-CD27^+$)					42.4	24.24-52.73	41.48	24.24-52.73
CD4 effector memory T (% of $CD4^+$) ($CD45RA^-CD27^-$)					**0.15**	3.40-11.17	**3**	3.40-11.17
CD4 TEMRA (% of $CD4^+$) ($CD45RA^+CD27^-$)					**0**	0.10-0.29	**0.07**	0.10-0.29
$CD8^+$ (/µl)					767	500-1200	1100	500-1200

$CD8^+$ (% of $CD3^+$)	61.07	21.01-33.94	**63.9**	21.01-33.94	**55.65**	21.01-33.94
CD8 naïve T (% of $CD8^+$) ($CD45RA^+CD27^+$)			48.10	41.41-73.04	59.74	41.41-73.04
CD8 central memory T (% of $CD8^+$) ($CD45RA^-CD27^+$)			21.10	13.21-37.89	13.50	13.21-37.89
CD8 effector memory T (% of $CD8^+$) ($CD45RA^-CD27^-$)			2.23	1.53-15.39	5.89	1.53-15.39
CD8 TEMRA (% of $CD8^+$) ($CD45RA^+CD27^-$)			**28.6**	2.01-21.65	20.87	2.01-21.65
NK cells						
$CD16^+CD56^+$ (/µl)			420	300-600	399	300-600
$CD16^+CD56^+$ (%)	**9.75**	10.01-26.98	24.26	10.01-26.98	20.23	10.01-26.98

UD, undetectable. TEMRA, EM re-expressing CD45RA. Boldface, out of range value. * Ig replacement therapy.

Table S4. Immunological features of patient 2

	11m	12m	Reference value
Serum Abs			
IgG (g/L)	**UD**		4.0-8.3
IgA (g/L)	**UD**		0.08-0.8
IgM (g/L)	**UD**		0.06-1.45
IgE (µg/L)	**UD**		<55
Corynebacterium diphtheriae toxin antibody	**UD** (<0.01 IU/mL)		Detectable
Clostridium tetani toxin antibody	**UD** (<0.01 IU/mL)		Detectable
B lymphocytes			
$CD19^+$ (/µl)	1140	1330	600-2700
$CD19^+$ (%)	0.23	0.23	0.15-0.39
Naïve B (% of $CD19^+$) (IgD^+CD27^-)	**95.2**		71-94
Switched memory B (% of $CD19^+$) ($IgM^-IgD^-CD27^+CD38^{low}$)	**0.2**		1-11
Un-switched memory B (% of $CD19^+$)	3.4		2-10
$CD21^{low}$ (% of $CD19^+$) ($CD38^{lo}CD21^{lo}$)	**0.2**		1-7
Transitional B (% of $CD19^+$) ($CD24^{hi}CD38^{hi}$)	**1.3**		8-27
T lymphocytes			
$CD3^+$ (/µl)	3740	4190	1600-6700
$CD3^+$ (%)	76	73	54-76
$CD4^+$ (/µl)	2820	3230	1000-4600
$CD4^+$ (% of $CD3^+$)	**59**	**56**	31-54
CD4 naïve T (% of $CD4^+$) ($CD45RA^+CCR7^+$)	75.7	73.3	54-80
CD4 central memory T (% of $CD4^+$) ($CD45RA^-CCR7^+$)	19.3	20	10-26

CD4 effector memory T (% of $CD4^+$) ($CD45RA^-CCR7^-$)	4.6	5.5	3-16
CD4 TEMRA (% of $CD4^+$) ($CD45RA^+CCR7^+$)	**0.5**	**1.2**	3-12
$CD8^+$ (/µl)	810	1030	400-2100
$CD8^+$ (% of $CD3^+$)	17	18	12-28
CD8 naïve T (% of $CD8^+$) ($CD45RA^+CCR7^+$)	66.90	**77.90**	34-73
CD8 central memory T (% of $CD8^+$) ($CD45RA^-CCR7^+$)	5.60	9.90	3-15
CD8 effector memory T (% of $CD8^+$) $CD45RA^-CCR7^-$)	26.4	9.3	9-47
CD8 TEMRA (% of $CD8^+$) ($CD45RA^+CCR7^+$)	**1.2**	**2.9**	7-25
NK cells			
$CD16^+CD56^+$ (/µl)	40	200	
$CD16^+CD56^+$ (%)	0.01	0.04	

UD, undetectable. TEMRA, EM re-expressing CD45RA. Boldface, out of range value.

Table S5. Immunological features of patient 3

	2.5m	1y9m	2y5m	3y4m	3y9m	Reference value	8y5m	8y9m	9y8m	Reference value
Serum Abs										
IgG (g/L)	**2**	4.63*	5.83*		10.66*	2.7-11.8	**12.54***	**13.6***	9.1*	5.82-11.54
IgA (g/L)	**<0.03**	**<0.05**	**0.05**		**0.06**	0.1-1.3	**0.17**	**0.15**	**0.36**	0.46-1.57
IgM (g/L)	**<0.02**	**<0.05**	**0.05**		**<0.05**	0.36-1.1	**<0.05**	**<0.05**	**<0.05**	0.54-1.55
IgE (kUI/L)	<2								15.7	(<148)
B lymphocytes										
$CD19^+$ (/µl)		598	527	**286**	**176**	390-1400	**90**	**91**	**109**	219-509
$CD19^+$ (%)		**13**	17	**10**	**8**	14-33	6	7	5	4.8-24.3
Naïve B (% of $CD19^+$) (IgD^+CD27^-)			**98**		**94**	78.5-84.6	**92**		**93**	58.5-84.6
Memory B (% of $CD19^+$) ($CD27^+$)		**1**	**1**		**3**	11.9-18.2	**8**		**7**	9-35
Memory B (% of $CD19^+$) (IgD^-CD27^+)			**0.3**		**1**	4.4-7.9	**1**		**0.6**	4.4-20.5
Switched memory B (% of $CD19^+$) ($IgM^-IgD^-CD27^+$)			**0.2**							
MZB-Like (% of $CD19^+$) (IgD^+CD27^+)		**1**	**1**		**1**	5.9-10.8	7		6	3-21.1
$CD21^{low}$ (% of $CD19^+$) ($CD38^{lo}CD21^{lo}$)		0.3	2		2					
Transitional B (% of $CD19^+$) ($CD24^{hi}CD21^{hi}$)		82	77							
T lymphocytes										
$CD3^+$ (/µl)		3358	2356	2485	1892	1400-3700	1332	**1146**	2005	1200-2600
$CD3^+$ (%)		73	**76**	**87**	**86**	56-75	**89**	**88**	**91**	60-76
$CD4^+$ (/µl)		**2300**	1643	1685	1232	700-2200	793	729	1383	650-1500
$CD4^+$ (% of $CD3^+$)		**50**	**53**	**59**	**56**	28-47	**53**	**56**	**63**	31-47
CD4 naïve T (% of $CD4^+$) ($CD45RA^+$)		86	82	85		73-86	**80.5**	**77**	67	58-70

CD4 naïve RTE (% of $CD4^+$)	**43**	**46**	**47**		57-65	52	47	44	43-55
($CD31^+CD45RA^+$)									
$CD8^+$ (/µl)	690	**465**	514	**374**	490-1300	389	**299**	490	370-1100
$CD8^+$ (% of $CD3^+$)	**15**	**15**	18	17	16-30	26	23	22	18-35
CD8 naïve T (% of $CD8^+$)	**87**	**91**	**95**		52-68	**84**	**85**	**94**	52-68
($CD45RA^+CCR7^+$)									
CD8 central memory T (% of $CD8^+$) ($CD45RA^-$ $CCR7^+$)	**7**	**5**	3		3-4	**1.5**	**5**	**1**	3-4
CD8 effector memory T (% of $CD8^+$) ($CD45RA^-$ $CCR7^-$)	**3**	**2**	**1**		11-20	**9**	**8**	**2**	11-20
CD8 TEMRA (% of $CD8^+$)	**3**	**2**	**1**		16-28	**5.5**	**2**	**2**	16-28
($CD45RA^+CCR7^-$)									
NK cells									
$CD16^+CD56^+$ (/µl)	598	186	**86**	**66**	130-720	**90**	**52**	**88**	100-480
$CD16^+CD56^+$ (%)	13	6	**3**	**3**	4-17	6	4	4	4-17

RTE, Recent thymus emigrant. TEMRA, EM re-expressing CD45RA. Boldface, out of range value. * Ig replacement therapy.

Table S6. Immunological features of patient 4

	1y5m	4y	Reference value
Serum Abs			
IgG (mg/dl)	**169**		685 (424-1051)
IgA (mg/dl)	**9**		47 (14-123)
IgM (mg/dl)	**6**		95 (48-168)
IgE (mg/dl)			
B lymphocytes			
$CD19^+$ (%)		**7.83**	11.12 (8.17-15.3)
Naïve B (% of $CD19^+$) (IgD^+CD27^-)		**92.3**	61.3 (44.9-77.5)
Switched memory B (% of $CD19^+$) (IgD^-CD27^+)		**1.22**	21.24 (10.4-30.4)
Un-switched memory B (% of $CD19^+$) (IgD^+CD27^+)		**4.27**	10.61 (3.62-22.2)
Transitional B (% of $CD19^+$) ($CD20^+CD38^{hi}$)		**9.46**	3.01 (1.73-4.08)
T lymphocytes			
$CD3^+$ (%)		53.6	60.26 (41.4-71.7)
$CD4^+$ (% of $CD3^+$)		**44.6**	59.6 (45.4-72.8)
CD4 naïve T (% of $CD4^+$) ($CD45RA^+CCR7^+$)		**96.3**	81.16 (72.5-91.5)
CD4 central memory T (% of $CD4^+$) ($CD45RA^-CCR7^+$)		**2.29**	14.8 (4.91-22.5)
CD4 effector memory T (% of $CD4^+$) ($CD45RA^-CCR7^-$)		**0.3**	1.226 (0.6-1.94)
CD4 TEMRA (% of $CD4^+$) ($CD45RA^+CCR7^+$)		**1.07**	2.824 (1.52-4.07)
$CD8^+$ (% of $CD3^+$)		**44.4**	31.68 (19.1-40.1)
CD8 naïve T (% of $CD8^+$) ($CD45RA^+CCR7^+$)		**94.4**	52.58 (36.3-69.9)

CD8 central memory T (% of $CD8^+$) ($CD45RA^-CCR7^+$)	**0.14**	4.38 (0.4-8.08)
CD8 effector memory T (% of $CD8^+$) $CD45RA^-CCR7^-$)	**0.29**	5.452 (1.87-7.48)
CD8 TEMRA (% of $CD8^+$) ($CD45RA^+CCR7^+$)	**5.14**	37.56 (27.8-48.9)
NK cells		
$CD16^+CD56^+$ (%)	19.2	10.552 (3.45-22.7)

TEMRA, EM re-expressing CD45RA. Boldface, out of range value.

Table S7. Immunological features of patient 5

	7.5m	Reference value	8m	Reference value	17y6m	Reference value
Serum Abs						
IgG (g/L)	**<0.35**	2.42-11.08			*	4.79-14.33
IgA (g/L)	0.07	0.02-1.26			**0.21**	0.6-2.3.49
IgM (g/L)	**<0.05**	0.21-2.15			**<0.19**	0.26-2.32
IgE (IU/ml)	7	2-34			ND	
B lymphocytes						
$CD19^+$ (/µl)			1590	130-6300	231	64-820
($IgM^{++}CD38^{++}$) (/µl)			**7**	15-1700	4	1-100
(IgM^+IgD^+) (/µl)			1557	110-5300	177	28-550
(IgD^+CD27^-) (/µl)			1573	461-1939	173	126-1939
Switched memory B (/µl) ($CD20^+IgM^-CD27^+$)			**0**	1.5-82	**0.6**	4.5-130
T lymphocytes						
$CD3^+$ (/µl)			2981	400-11500	1201	780-3000
$CD3^+DR^+$ (/µl)			**497**	135-232	89	73-162
$CD3^+TCR\alpha/\beta^+$ (/µl)			2881	1200-11500	1140	600-3300
$CD3^+TCR\gamma/\delta^+$ (/µl)			99	38-890	37	25-200
$CD3^+CD4^+$ (/µl)			1689	1000-7200	801	500-2000
CD4 naïve T (/µl) ($CD4^+CD45RA^+CCR7^+$)			1165	800-7600	432	199-2300
CD4 central memory T (/µl) ($CD4^+CD45RO^+CCR7^+$)			219	83-1300	**57**	180-1100
CD4 effector memory T (/µl) ($CD4^+CD45RO^+CCR7^-$)			**253**	1-72	184	13-220
CD4 TEMRA (/µl) ($CD4^+CD45RA^+CCR7^-$)			51	1-400	27	1-68
$CD8^+$ (/µl)			1143	200-5400	339	200-1200
CD8 naïve T (/µl) ($CD8^+CD45RA^+CCR7^+$)			503	150-3200	247	16-1000

CD8 central memory T (/µl) ($CD8^+CD45RO^+CCR7^+$)	45	2-150	**4**	5-120
CD8 effector memory T (/µl) ($CD8^+CD45RO^+CCR7^-$)	388	8-1400	**34**	40-640
CD8 TEMRA (/µl) ($CD8^+CD45RA^+CCR7^-$)	205	17-280	44	25-280
NK cells (/µl) ($CD3^-CD16^+CD56^+$)	248	68-3900	**31**	100-1200
NKT cells (/µl) ($CD3^+CD16^+CD56^+$)	0	4.4-510	**12**	23-410

TEMRA, EM re-expressing CD45RA. Boldface, out of range value. * Ig replacement therapy.

Table S8. Immunological features of patient 6

	8y	Reference value
Serum Abs		
IgG (g/L)	**1.54**	5.14-16.72
IgA (g/L)	**<0.05**	0.52-2.26
IgM (g/L)	**<0.05**	0.16-1.88
IgE (IU/ml)	8	2-403
B lymphocytes		
$CD19^+$ (/µl)	201	100-800
Switched memory B (/µl) ($CD20^+IgM^-CD27^+$)	**4**	7-51
T lymphocytes		
$CD3^+$ (/µl)	2936	770-4000
$CD3^+CD4^+$ (/µl)	1805	400-2500
CD4 naïve T (/µl) ($CD4^+CD45RA^+CD62L^+$)	1451	200-2500
CD4 central memory T (/µl) ($CD4^+CD45RA^-CD62L^+$)	131	4-510
CD4 effector memory T (/µl) ($CD4^+CD45RA^-CD62L^-$)	138	3-170
CD4 TEMRA (/µl) ($CD4^+CD45RA^+CD62L^-$)	**86**	1-25
$CD8^+$ (/µl)	921	200-1700
CD8 naïve T (/µl) ($CD8^+CD45RA^+CD62L^+$)	339	42-1300
CD8 central memory T (/µl) ($CD8^+CD45RA^-CD62L^+$)	**48**	6-43
CD8 effector memory T (/µl) ($CD8^+CD45RA^-CD62L^-$)	187	45-410
CD8 TEMRA (/µl) ($CD8^+CD45RA^+CD62L^-$)	**347**	57-340
NK cells (/µl) ($CD3^-CD16^+$ and/or $CD56^+$)	**593**	70-590

NKT cells (/μl) ($CD3^+CD16^+$ and/or $CD56^+$)	336	12-340

UD, undetectable. TEMRA, EM re-expressing CD45RA. Boldface, out of range value.

Table S9. Immunological features of patient 7

	3y	Reference value
Serum Abs		
IgG (g/L)	**0.24**	4.85-11.60
IgA (g/L)	**<0.05**	0.14-2.12
IgM (g/L)	**<0.05**	0.26-1.55
IgE (IU/ml)	2	2-307
B lymphocytes		
$CD19^+$ (/µl)	222	180-1300
Switched memory B (/µl) ($CD20^+IgM^-CD27^+$)	3	2.2-25
T lymphocytes		
$CD3^+$ (/µl)	2538	850-4300
$CD3^+CD4^+$ (/µl)	991	500-2700
CD4 naïve T (/µl) ($CD4^+CD45RA^+CD62L^+$)	664	300-2300
CD4 central memory T (/µl) ($CD4^+CD45RA^-CD62L^+$)	**76**	160-660
CD4 effector memory T (/µl) ($CD4^+CD45RA^-CD62L^-$)	**155**	4-89
CD4 TEMRA (/µl) ($CD4^+CD45RA^+CD62L^-$)	**116**	1-16
$CD8^+$ (/µl)	1404	200-1800
CD8 naïve T (/µl) ($CD8^+CD45RA^+CD62L^+$)	261	53-1100
CD8 central memory T (/µl) ($CD8^+CD45RA^-CD62L^+$)	21	4-64
CD8 effector memory T (/µl) ($CD8^+CD45RA^-CD62L^-$)	**745**	24-590
CD8 TEMRA (/µl) ($CD8^+CD45RA^+CD62L^-$)	377	25-530
NK cells (/µl) ($CD3^-CD16^+$ and/or $CD56^+$)	289	61-510

NKT cells (/μl) ($CD3^+CD16^+$ and/or $CD56^+$)	**322**	15-250

TEMRA, EM re-expressing CD45RA. Boldface, out of range value.

Table S10. Th cell subset distributions in T95R patients and HC

	HC	HC	P1	HC	HC	HC	HC	P2	P2	P2	P2
Age	12y	12y	12y	3y	3y	3y	3y	2y	2y	2y	2y
Tfh (% of CD4+)	2.82	3.38	3.61	4.04	2.2	6.86	1.81	1.8	1.9	2.77	1.1
Th1 (% of CD4+)	0.52	0.22	2.7	2	4	4	4	1	2	1.4	2
Th2 (% of CD4+)	0.51	0.39	0.99								
Th17 (% of CD4+)	1.75	1.62	1.32								
Treg (% of CD4+)		4.99	7.29								
Tfr (% of CD4+)											

	HC	HC	HC	HC	HC	P3	P4	HC	HC	HC	P5	P5	P5	P6	P7
Age	NA	39y	31y	18y8m	2y	9y	4y	4y11m	6y10m	9y8m	9m	1y2m	1y9m	8y	3y
Tfh (% of CD4+)	22.3	16.3	18.3	1.39	9.8	3.6	2.46	5.39	4.27	0.66	1.70	1.71	1.28	2.27	3.03
Th1 (% of CD4+)	8.44	6.97	9.25	6.48	7.89	17.3	10.5	8.0	5.1	7.2	10.3	9.9	13.0	3.66	9.65
Th2 (% of CD4+)	3.64	5.4	4.12	9.39	2.96	1.6	3.73	1.5	1.3	1.7	0.6	2.2	1.3	0.6	1.08
Th17 (% of CD4+)	5.28	6	5.27	4.94	5.1	0.97	2.76	0.8	0.5	2.7	0	0	0.1	0.34	0.3
Treg (% of CD4+)	4.69	3.12	5.36	1.6	3.02	2.06	1.51	6.36	6.18	8.87	5.25	7.42	9.64	2.49	1.51
Tfr (% of CD4+)								0.19	0.49	0.22	0.23	0.55	0.24		

Th-cell subsets of P1-P4, P6-P7 and their corresponding HC were determined by surface chemokine receptor staining, P5 and corresponding HC were determined by intracellular cytokine staining. P1, P2, and P5-P7 were analyzed by flow cytometry and P3 and P4 by CyTOF.

NA, not available.

Table S11. Monocyte subset distributions in T95R patients and HC

	HC	HC	HC	P2	P2	P2	HC	HC	HC	HC	HC	P3	P4
Age	3y	3y	3y	2y	2y	2y	NA	39y	31y	18y8m	2y	9y	4y
Classical monocytes (% of monocytes)	67.4	70.7	65	32.7	16.4	30.6	76.8	57.9	70.1	74.6	58.9	65.5	78.4
Intermediate monocytes (% of monocytes)							7.27	30.2	18.4	8.65	16.4	7.6	12
Non-classical monocytes (% of monocytes)	5.6	3	4	4	5	6	2.52	2.22	4.98	3.43	4.52	1.64	0.38

	HC	HC	HC	HC	HC	P5
Age	12y	18y	18y	18y	20y	17y6m
Classical monocytes (% of monocytes)	78.7	72.6	82.5	81.3	83.4	94.3
Intermediate monocytes (% of monocytes)	10.4	9.4	4.0	4.8	6.1	1.9
Non-classical monocytes (% of monocytes)	6.1	10.5	8.5	10.1	4.1	0.3

P2 and P5 were analyzed by flow cytometry and P3 and P4 by CyTOF. NA, not available.

Table S12. List of antibodies and stimuli used in the present study

REAGENT or RESOURCE	COMPANY	IDENTIFIER
Antibodies		
Percp/Cy5.5 Anti-human CD38 Clone HIT2	BD Biosciences	561106
PE/Cy7 Anti-human CD38 Clone HIT2	Biolegend	303515
APC Anti-human CD19 Clone HIB19	Biolegend	302212
PE/Cy7 Anti-human IgG Clone G18-145	BD Biosciences	561298
PE Anti-human IgD Clone IA6-2	BD Biosciences	555779
APC/Cy7 Anti-human CD27 Clone O323	Biolegend	356424
FITC Anti-human CD20 Clone 2H7	Biolegend	302304
PE Anti-human HLADR Clone G46-6	BD Biosciences	556644
PE/Cy7 Anti-human CD69 Clone FN50	BD Biosciences	557745
FITC Anti-human CD80 Clone L307.4	BD Biosciences	557226
APC Anti-human CD86 Clone IT2.2	Biolegend	305412
PE Anti-human CD25 Clone 24212	R&D	FAB1020P
PE Anti-human CD24 Clone ML5	BD Biosciences	555428
APC-H7 Anti-human CD3 Clone SK7	BD Biosciences	560176
Percp/Cy5.5 Anti-human CD3 Clone SK7	BD Biosciences	340949
FITC Anti-human CD4 Clone RPA-T4	BD Biosciences	555346
BV510 Anti-human CD8 Clone RPA-T8	BD Biosciences	563256
APC Anti-human CD8a Clone RPA-T8	Biolegend	301049
PE/Cy7 Anti-human CD45RA Clone HI30	BD Biosciences	557748
APC Anti-human CD27 Clone M-T271	BD Biosciences	558664
PE-Cy7 Anti-human CD138	Biolegend	356513
Percp/Cy5.5 Anti-human CD38	Biolegend	356614
PE Anti-human CD27	Biolegend	356406

Alexa Fluor 647 Anti-human BCMA	Biolegend	357506
APC/Cy7 Anti-human CD19	Biolegend	302218
Alexa Fluor 647 Goat F(ab′)2 anti-human IgA	Jackson ImmunoResearch	109-496-011
PerCP Anti-human CD3	BD Biosciences	345766
PE Anti-human CD4	Biolegend	300508
APC Anti-human CD45RA	BD Biosciences	550855
PerCP Anti-human CXCR5	Thermo Fisher Scientific	46-9185-42
APC Anti-human PD-1	Thermo Fisher Scientific	17-9969-42
FITC Anti-human CD127	Biolegend	351312
Pacific Blue Anti-human CCR7	Biolegend	353210
APC Anti-human CD3	Beckman Coulter	IM2467
APC Alexa Fluor 750 Anti-human CD4	Beckman Coulter	A94682
APC-Alexa Fluor 700 Anti-human CD8	Beckman Coulter	B49181
Pacific Blue Anti-human CD8	Beckman Coulter	B49182
FITC Anti-human CD14	Dako/ Agilent	F0844
ECD Anti-human CD16	Beckman Coulter	B49216
APC-Alexa Fluor 700 Anti-human CD19	Beckman Coulter	B49212
PerCP Anti-human CD20	Biolegend	302324
Horizon V450 Anti-human CD27	Becton Dickinson	560448
PE-Cy7 Anti-human CD38	Becton Dickinson	335825
Krome-Orange Anti-human CD45	Beckman Coulter	B36294
PE-Cy7 Anti-human CD45RA	Beckman Coulter	B10821
FITC Anti-human CD45RO	Dako/ Agilent	F0800
ECD Anti-human CD56	Beckman Coulter	B49214
FITC Anti-human CD107a	Becton Dickinson	555800
PE Anti-human HLA-DR	Beckman Coulter	IM1639

FITC Anti-human IgD	Dako/ Agilent	F0189
APC Anti-human IgM	Biolegend	314510
PE-Cy7 Anti-human IL-4	Biolegend	500824
eFlour 450 Anti-human IL-17A	eBioscience (Thermo Fisher Scientific)	48-7179-42
FITC Anti-human IFN-g	Biolegend	502506
Anti-Human FOXP3 Staining Set PE	Thermo Fisher Scientific	72-5774-40
Human regulatory T-cell staining Kit #3	eBioscience (Thermo Fisher Scientific)	88-8995-41
Beta Mark TCR Vbeta Repertoire Kit	Beckman Coulter	IM3497
TruStain FcX	Biolegend	101320
PerCP/cy5.5 Anti-mouse B220	Biolegend	103235
PE Anti-mouse B220	Biolegend	102504
APC Anti-Mouse CD138 Clone 281-2	BD Biosciences	558626
PE-Cy7 Anti-Mouse CD45R/B220 Clone RA3-6B2	BD Biosciences	553093
APC Anti-Mouse CD38 Clone 90	Biolegend	102712
FITC Anti-Mouse FAS Clone Jo2	BD Biosciences	554257
APC-Cy7 Anti-Mouse CD3 Clone 17A2	Biolegend	100221
FITC Anti-Mouse CD4 Clone H129.19	BD Biosciences	553650
PE-Cy7 Anti-Mouse CD8 Clone RPA-T8	Biolegend	301012
PE Anti-Mouse CD44 Clone 2M7	BD Biosciences	553134
APC Anti-Mouse CD62L Clone MEL-14	BD Biosciences	553152
PE Anti-mouse IgA Clone mA-6E1	eBioscience	12-4204-82
BUV737 Anti-Human CD19	BD Biosciences	741829
BUV615 Anti-Human IgD	BD Biosciences	751595
BV605 Anti-Human CD27	BD Biosciences	751673
APC Anti-Human CD38	BD Biosciences	560980

BV421 Anti-Human HLA-DR	BioLegend	307635
BV750 Anti-Human CD14	BD Biosciences	746920
BUV496 Anti-Human CD16	BD Biosciences	612945
BB660 Anti-Human CD11c	BD Biosciences	Custom
BUV661 Anti-Human CD56	BD Biosciences	750478
Fixable Viability Dye eFluor 780	BD Biosciences	565388
BV510 Anti-Human CD3	BD Biosciences	563109
BUV395 Anti-Human CD4	BD Biosciences	563550
BV570 Anti-Human CD8	BioLegend	301037
BV510 Anti-Human IgM	BD Biosciences	563113
BUV395 Anti-Human TNFα	BD Biosciences	563996
BV711 Anti-Human IFNγ	BD Biosciences	564793
PerCp-Cy5.5 Anti-Human CD45RA	BD Biosciences	563429
BV421 Anti-Human CXCR5	BD Biosciences	562747
BV786 Anti-Human ICOS	BD Biosciences	741017
PE Anti-Human IRF4	BD Biosciences	566649
BV650 Anti-Human IL2	BD Biosciences	564166
Alexa Fluor® 647 anti-IRF4 Antibody	BioLegend	646408
V450 Mouse Anti-Human IL-4	BD	561595
PE anti-human IFN-γ Antibody	Biolegend	506507
Alexa Fluor® 647 Mouse anti-Human IL-17A	BD	560491
APC Mouse Anti-Human CD4; RPA-T4	BD	555349
FITC Mouse Anti-Human CD8; RPA-T8	BD	555366
APC/Cyanine 7 anti-human CD19; HIP19	Biolegend	302218
7-amino-actinomycin D	Invitrogen	00-6993-50
Anti-IRF4 antibody (E8H3S)	Cell Signaling Technology	62834

Anti-IRF4 antibody (P173)	Cell Signaling Technology	4948
Anti-IRF4 antibody	Cell Signaling Technology	4964S
Anti-β-actin antibody	Cell Signaling Technology	3700S
Anti-GAPDH antibody	Cell Signaling Technology	2118S
Anti-Lamin B antibody	Santa Cruz Biotechnology	Sc-6216
IRDye 680RD Goat anti-Mouse	LI-COR Bioscience	925-68070
IRDye 800CW Goat anti-Rabbit	LI-COR Bioscience	926-32211
Anti-PARP antibody (46D11)	Cell Signaling Technology	9532
Anti-DYKDDDDK Tag antibody	Cell Signaling Technology	2368
Anti-Flag antibody (M2)	Sigma	F1804
Anti-HA antibody (C29F4)	Cell Signaling Technology	3724
Normal rabbit IgG antibody	Cell Signaling Technology	2729
Anti-AID antibody (L7E7)	Cell Signaling Technology	4975
Anti-β-actin antibody	Sigma	A1978
Anti-Vinculin	Santa Cruz	sc-73614
Rabbit monoclonal to human GAPDH	Abcam	ab181602
Rabbit monoclonal to MUM1 (IRF4)	Abcam	ab124691
Goat anti-rabbit IgG (H+L)-HRP conjugate	BioRad	170-6515
Mouse monoclonal to human CD20 (L26)	Dako	M0755
Mouse monoclonal to human CD38 (SPC32)	Leica Biosystems	NCL-CD38-290
Mouse monoclonal to human CD138 (MI15)	Dako	7228
Mouse monoclonal to human IRF4/ MUM1 (MUM1p)	Dako	7259
Goat Anti-Human Ig-UNLB	SouthernBiotech	2010-01
Goat Anti-Human IgM-BIOT	SouthernBiotech	2020-08
Goat Anti-Human IgG-BIOT	SouthernBiotech	2040-08

Human IgM Lambda-UNLB	SouthernBiotech	0158L-01
Human IgG-UNLB	SouthernBiotech	0150-01
HRP Avidin	Biolegend	405103
Neutralite Avidin-AP	SouthernBiotech	7200-04
Purified NA/LE Mouse Anti-Human CD3	BD Biosciences	555336
Purified NA/LE Mouse Anti-Human CD28	BD Biosciences	555725
F(ab')2 anti-human IgM	SouthernBiotech	2022-14
Mouse IgA-UNLB	SouthernBiotech	0106-01
Mouse IgM-UNLB	SouthernBiotech	0101-01
Mouse IgG-UNLB	SouthernBiotech	0107-01
Mouse IgG_1-UNLB	SouthernBiotech	0102-01
Mouse IgG_{2b}-UNLB	SouthernBiotech	0104-01
Mouse IgG_{2c}-UNLB	SouthernBiotech	0122-01
Mouse IgG_3-UNLB	SouthernBiotech	0105-01
Anti-mouse Ig-UNLB	SouthernBiotech	1010-01
Goat Anti-Mouse IgA-HRP	SouthernBiotech	1040-05
Goat Anti-Mouse IgM-HRP	SouthernBiotech	1020-05
Goat Anti-Mouse IgG-HRP	SouthernBiotech	1030-05
Goat Anti-Mouse IgG_1, Human ads-HRP	SouthernBiotech	1070-05
Goat Anti-Mouse IgG_{2b}, Human ads-HRP	SouthernBiotech	1090-05
Goat Anti-Mouse IgG_{2c}-HRP	SouthernBiotech	1078-05
Goat Anti-Mouse IgG_3, Human ads-HRP	SouthernBiotech	1100-05
Goat Anti-Mouse IgG_1-AP	SouthernBiotech	1071-04
Peroxidase-AffiniPure Goat Anti-Rabbit IgG (H+L)	Jackson Immunoresearch	111-035-003
Chemicals, Peptides, and Recombinant Proteins		

Recombinant Human IL2 GMP Protein, Carrier free	R&D	202-GMP-010
Recombinant Human IL4	BD Biosciences	554605
CpG ODN 2006	Sangon Biotech	NA
CpG ODN 2006	ENZO	ALX 746-006-C100
Recombinant Mouse IL4	R&D	404-ML-010
Recombinant Mouse IL21	Biolegend	574502
MEGACD40L® Protein	ENZO	ALX-522-110-C010
IL21	Peprotech	200-21
IL2	Peprotech	200-02
IL4	Peprotech	200-04
Anti-Human IgM	Jackson Immunoresearch	109-006-129
Anti-CD3	eBioscience	16-0037-85
Anti-CD28	eBioscience	16-0289-85
Phorbol 12-myristate 13-acetate (PMA)	Sigma	P8139
Brefeldin A	Sigma	B7651
Ionomycin	Thermo Fisher Scientific	I24222
LPS (E. coli O111:B4)	Sigma-Aldrich	L4391/L2880
CD40L		NA

Table S13. List of oligonucleotides used in the current study

Primers for mutation confirmation		
IRF4-for P1	Forward	AGGACCTATGCGCCATTCTT
	Reverse	GGCAGGCAGGCAATACAAAA
humIRF4_gDNA_Ex1	Forward	AAGTCCCTCTCCCCAGTC
	Reverse	ACCTCTGGTTCGCGCTC
humIRF4_gDNA_Ex2	Forward	CCTCGTGGTCACTGGCGC
	Reverse	CCTCCTCCTGCGGCTCCG
humIRF4_gDNA_Ex3	Forward	TGGGCAGCAGAGCAGGAC
	Reverse	TAAGGTGCCTCAAGGATCTG
humIRF4_gDNA_Ex4	Forward	AACACCGTGTTATGCATTCT
	Reverse	CTGGGCTGCTGTGGTTCTC
humIRF4_gDNA_Ex5	Forward	GATGATAAAATGCTTCGGCTG
	Reverse	GGAAAGAGCTTTGGTGCTG
humIRF4_gDNA_Ex6	Forward	TCCCAGGCTTCACACACAC
	Reverse	CTAAAGTCCCATCGAATCTGC
humIRF4_gDNA_Ex7	Forward	AGGTGCTTGGCTCTGTGGAG
	Reverse	CAGGAGGAAGACCTCAGCC
humIRF4_gDNA_Ex8	Forward	TTCACATCAAGAGCCCCAC
	Reverse	TTCTAAATGAAACTCTGGCC
humIRF4_gDNA_Ex9	Forward	TTCTAGGATGTAACTTTGGGC
	Reverse	CCTGGGAGACAGAGCAAGAC
Primers for RT-PCR		
ACTBcDNA	Forward	CCAACACAGTGCTGTCTG
	Reverse	CAACTAAGTCATAGTCCACC
IRF4cDNA	Forward	GGGAAGCTCCGCCAGTGG
	Reverse	GGGTAAGGCGTTGTCATGGTG
gRNA for IRF4 CRISPR/CAS9		

#1 gRNA	Oligo1	CACCGCAAGCAGGACTACAACCGCG
	Oligo2	AAACCGCGGTTGTAGTCCTGCTTGC
#2 gRNA	Oligo1	CACCGCCACCTGGAAGACGCGCCTG
	Oligo2	AAACCAGGCGCGTCTTCCAGGTGGC
Primers for vector generation		
IRF4	Forward	CGGGGATCCCCACCATGAACCTGGAGGGCGGC
	Reverse	CGGGGATCCTCATTCTTGAATAGAGGAATGGC
	dAR-Reverse	CCGGAATTCTCATTGTTGAGCAAAATAATATAG TTGT
IRF4-FLAG	Forward	CCGGAATTCCCACCATGAACCTGGAGGGCGGC
	Reverse	CGGGGATCCTCA CTTATCGTCGTCATCCTTGTAATC TTCTTGAATAGAGGAATGGC
IRF4-HA	Forward	CCGGAATTCCCACCATGAACCTGGAGGGCGGC
	Reverse	CGGGGATCCTCA CTTATCGTCGTCATCCTTGTAATC TTCTTGAATAGAGGAATGGC
pGL3-Basic	PromF	TAGTACTAACATACGCTCTCCATC
Primer for QPCR		
hIRF4	Forward	TCCGAGAAGGCATCGACAAG
	Reverse	AGGCGTTGTCATGGTGTAGG
hPRDM1	Forward	GCAACTGGATGCGCTATGTG
	Reverse	TCTCAGTGCTCGGTTGCTTT
hXBP1	Forward	TTCCGGAGCTGGGTATCTCA
	Reverse	GAAAGGGAACCCCCGTATCC
hACTIN	Forward	AGCGAGCATCCCCCAAAGTT
	Reverse	GGGCACGAAGGCTCATCATT
mAID	Forward	TGGACAGCCTTCTGATGA
	Reverse	GTCTGAGATGTAGCGTAGG

mGAPDH	Forward	TGTGAACGGATTTGGCCGTA
	Reverse	ACTGTGCCGTTGAATTTGCC
gBlock DNA Fragment for luciferase assay		
CXCL13NewA wt / B wt		AGAATATACGTTCTTATCTGCAATCTTCTCATCTAAAATTGACCACACGCTCAGTCATAAAGCAAGTCTTAAAATCAAAAATATCAATATTAAGCATCTTCTCACACCACAGTGAAATAAAAATAGAAATTAATATCAAAAGGAACTCTCAAAATGACACAAATATATGGAAACAAAACAACTTCTGAATTACTTTTGGGT
Probes for EMSA		
ISRE 3xGAAA	Forward	5'IRDye700-gatcGGGAAAGGGAAACCGAAACTGAA
	Reverse	TTCAGTTTCGGTTTCCCTTTCCCgatc
ISRE 3xGATA	Forward	5'IRDye700-gatcGGGATAGGGATACCGATACTGAA
	Reverse	TTCAGTATCGGTATCCCTATCCCgatc
EMSA_ISRE_3xGAAA	Forward	AGC TGG GAA AGG GAA ACC GAA ACT G
	Reverse	AGC TCA GTT TCG GTT TCC CTT TCC C
EMSA_EICE	Forward	AGCTATAAAAGGAAGTGAAACCAAG
	Reverse	AGCTCTTGGTTTCACTTCCTTTTAT
EMSA_EICE_mut+1A	Forward	AGCTATAAAAGGAAGTGAAAACAAG
	Reverse	AGCTCTTGTTTTCACTTCCTTTTAT
EMSA_EICE_IgK3_enhancer	Forward	ACGTAAGACCCTTTGAGGAACTGAAAACAGAACC
	Reverse	AGCTGGTTCTGTTTTCAGTTCCTCAAAGGGTCTT
EMSA_EICE_Igk3_enhancer_mut+1C	Forward	ACGTAAGACCCTTTGAGGAACTGAAACCAGAACC
	Reverse	AGCTGGTTCTGGTTTCAGTTCCTCAAAGGGTCTT
EMSA_CXCL13_A	Forward	AGCTACGCTCAGTCATAAAGCAAGTCT
	Reverse	AGCTAGACTTGCTTTATGACTGAGCGT

EMSA_CXCL13_B	Forward	AGCTAGGAACTCTCAAAATGACACAAA
	Reverse	AGCTTTTGTGTCATTTTGAGAGTTCCT
EMSA_CXCL13_C	Forward	AGCTACTGTGTCATATTGACTCTTAAA
	Reverse	AGCTTTTAAGAGTCAATATGACACAGT